# Role of the SWI/SNF Chromatin Remodelling Complex in the Axon Development of the Drosophila Mushroom Body

Melissa C. Chubak, *The University of Western Ontario*

Supervisor: Dr. Jamie Kramer, *The University of Western Ontario*
A thesis submitted in partial fulfillment of the requirements for the Master of Science degree in Developmental Biology
© Melissa C. Chubak 2017

# Abstract

The SWI/SNF complex is an evolutionarily conserved ATP-dependent chromatin remodelling complex that has been implicated in the aetiology of intellectual disability (ID). Among the dominant ID genes, the SWI/SNF complex is the most highly enriched protein complex. However, its role in the nervous system is not yet understood. I systematically investigated the role of this complex in the development of the *Drosophila* mushroom body (MB), a complex brain structure required for learning and memory. Gross MB morphology was assessed using confocal microscopy to identify morphological defects following RNAi-mediated knockdown of the 15 individual SWI/SNF genes in the MB. Knockdown of several SWI/SNF genes resulted in morphological abnormalities that suggest a role for this protein complex in axon remodelling. These findings reveal a novel role for the SWI/SNF complex in axon development and pave the way for understanding the underlying gene regulatory mechanisms.

## Keywords

# Co-Authorship Statement

This project was conducted under the supervision of Dr. Jamie M. Kramer. All aspects of the experimental design and analysis were planned in cooperation with Dr. Kramer. The lethality assay was conducted in association with my fellow graduate student, Max Stone. With the exception of the lethality assay, all experiments were conducted by myself.

# Acknowledgments

First and foremost, I would like to thank Dr. Jamie Kramer for all of the guidance, encouragement and support he provided throughout my time in the program. Your passion for science is inspiring, and I am extremely grateful to have had the opportunity to work with a supervisor who cared so deeply about the success of his students.

I must acknowledge everyone who works at the Biotron's integrated microscopy facility. Specifically, I would like to thank Karen Nygard for providing valuable training and assistance on the confocal microscope. The success of this project would not have been possible without your help. I would also like to thank my committee members, Dr. Kathleen Hill and Dr. Anthony Percival-Smith for the valuable feedback and direction they provided over the course of my degree.

I would like to give a big thank you to each and every member of the Kramer lab – past and present. However, a special thank you goes out to Max Stone, Kevin Nixon, Spencer Jones and Taylor Lyons. I am so lucky to have been able to complete my degree in a lab with such great people, and I appreciate all of your suggestions, encouragement and good humour. Thank you for making the past two years enjoyable. Finally, I would like to thank my parents for their continued support throughout my academic endeavours. This would not have been possible without your love and support.

# Table of Contents

# List of Tables

# List of Figures

# List of Appendices

# List of Abbreviations

φC31          Site-specific recombinase from the PhiC31 bacteriophage

ALH           After larval hatching

ANOVA         Analysis of variance

ATP           Adenosine triphosphate

BAF           BRG1- or HBRM-associated factors

BAP           Brahma-associated protein

*BCL7-like*   *BCL Tumor Suppressor like-7*

BDSC          Bloomington *Drosophila* Stock Center

*BRG1*        *Brahma-related gene 1*

*BRM*         *Brahma*

ChIP          Chromatin immunoprecipitation

da            Dendrite arborization

DHR3          *Drosophila* hormone receptor 3

DIOPT         *Drosophila* RNAi Screening Center integrative ortholog prediction tool

DNA           Deoxyribonucleic acid

dsRNA         Double-stranded RNA

*e(y)3*       *enhancer of yellow 3*

EcR           Ecdysone receptor

esBAF         Embryonic stem cell BAF

GAL4          Galactose responsive transcription factor GAL4

GFP           Green fluorescent protein

H3K4          Lysine 4 of histone H3

*Hr39*        *Hormone receptor-like in 39*

ID            Intellectual disability

| | |
|---|---|
| IQ | Intelligence quotient |
| MB | Mushroom body |
| *MeCP2* | *Methyl-CpG-binding protein 2* |
| miR | microRNA |
| *mor* | *moira* |
| mRNA | Messenger RNA |
| nBAF | Neuronal BAF |
| NHL | Newly hatched larvae |
| npBAF | Neuronal progenitor BAF |
| PBAP | Polybromo-associated BAP |
| qPCR | Quantitative real-time polymerase chain reaction |
| RISC | RNA-induced silencing complex |
| RNA | Ribonucleic acid |
| RNAi | RNA interference |
| SAYP | Supporter of activation of yellow protein |
| siRNA | Short-interfering RNA |
| *Snr1* | *Snf5-related 1* |
| SWI/SNF | SWItch/Sucrose Non-Fermentable |
| TGF-β | Transforming growth factor beta-1 |
| TRiP | Transgenic RNAi Project |
| UAS | Upstream activating sequence |
| USP | Ultraspiracle protein |
| VDRC | Vienna *Drosophila* Stock Centre |

Chapter 1

# 1 INTRODUCTION

In both vertebrates and invertebrates, nervous system development involves the establishment of precise connections between neurons and their target cells. The ability of neurons to make these connections is mediated by several processes including axon guidance, pruning and synapse formation (Araújo & Tear, 2003; Luo & O'Leary, 2005; Munno & Syed, 2003). The intricate neuronal connections formed by these interactions are essential for nervous system functioning, and the ability to remodel these connections throughout life represents one of the most important features of the nervous system. Neuronal remodelling occurs throughout development in order to establish the mature pattern of dendrites and axons in the adult brain. However, the neurons of the adult brain continue to remodel their connections in response to changes in neuronal activity and the environment (Fuchs et al., 2014). Proper nervous system development and function is reliant on the coordinated efforts of transcription factors and epigenetic regulatory complexes to direct a precisely regulated program of gene expression (Hsieh & Gage, 2005). In this thesis, I investigate the role of the SWI/SNF (SWItch/Sucrose Non-Fermentable) chromatin remodelling complex in the axon development of the mushroom body (MB) in *Drosophila melanogaster*.

## 1.1 Epigenetic regulation in the nervous system

Broadly defined, "epigenetics" refers to changes in gene expression that are independent of the underlying DNA sequence (Berger et al., 2009). The term epigenetics was coined by C.H. Waddington, a developmental biologist who sought the mechanisms that allow genetically identical cells to develop into a myriad of radically different cell types (Waddington, 2012). In eukaryotes, DNA is tightly packaged into chromatin. The basic structural unit of chromatin is the nucleosome, consisting of approximately 147 base pairs of DNA wrapped around a histone octamer (Luger et al., 1997). In addition to packaging the DNA, nucleosomes play an important role in the regulation of gene expression. Nucleosomes are highly dynamic, and their state of compaction is critical in determining whether the transcriptional machinery is able to access the DNA for gene activation (Schones

et al., 2008). Nucleosome positioning is directed by various biochemical modifications which promote the condensation or relaxation of the chromatin structure, leading to the repression or activation of gene expression. These modifications include DNA methylation, post translational histone modifications and ATP-dependent chromatin remodelling (Goldberg et al., 2007). Among these mechanisms, DNA methylation and histone modifications are two of the most well studied. DNA methylation is typically associated with gene silencing (Medvedeva et al., 2014), whereas histone modifications both activate and repress gene transcription at various loci (Barski et al., 2007). Although the role of nucleosome remodelling has not been extensively characterized, ATP-dependent chromatin remodelling complexes are thought to play a key role in the regulation of gene expression by altering the accessibility of DNA to the transcriptional machinery (Vignali et al., 2000).

Epigenetic mechanisms were traditionally thought to be stable and heritable throughout meiosis and mitosis. However, studies have now shown that chromatin modifications can be highly dynamic in post-mitotic neurons (Olave et al., 2002; Rudenko & Tsai, 2014). The study of post-mitotic epigenetic regulatory mechanisms in neurons is termed neuroepigenetics (Sweatt, 2013). Epigenetic mechanisms have been found to play a key role in a number of neurological processes, including stress response (Weaver et al., 2004), adult neurogenesis (Lessard et al., 2007; Yoo et al., 2009) and memory formation (Gupta et al., 2010; Miller et al., 2008; Miller & Sweatt, 2007). For example, epigenetic regulation mediated by the methyl-CpG-binding protein 2 (*MeCP2*) is required for normal human brain development. The MeCP2 protein functions as a transcriptional repressor that mediates gene silencing through binding to regions of methylated DNA (Nan et al., 1997). Mice containing a null mutation in the *Mecp2* gene exhibit decreased spine density and a reduction in the number of dendritic branches (Kishi & Macklis, 2004; Smrt et al., 2007). A similar phenotype is observed following overexpression of the Mecp2 protein, indicating that neuronal maturation is dependent on the precise regulation of Mecp2 expression (Zhou et al., 2006). Furthermore, several studies suggest that histone modifications play an essential role in the nervous system. A study in flies revealed that the histone methyltransferase, G9a, is involved in the regulation of type 4 multidendritic sensory neurons, non-associative learning and courtship memory (Kramer et al., 2011). In addition, histone methyltransferase activity is required for the regulation of long term potentiation in the hippocampus (Gupta et al., 2010). Contextual fear conditioning experiments in rats revealed that the trimethylation of

histone 3 at lysine 4 (H3K4) was up regulated in the hippocampus during memory consolidation (Gupta et al., 2010). Moreover, mice deficient in the H3K4-specific methyltransferase, mixed-lineage leukemia (*Mll*), had severe deficits in their ability to form long term memories (Gupta et al., 2010). In addition to the examples provided here, numerous other studies have revealed a role for epigenetic mechanisms in the nervous system (Delgado-Morales et al., 2017; Jiang et al., 2008; Levine et al., 2005). Together, these findings indicate that epigenetic mechanisms play an important role in the regulation of neuronal gene expression. However, despite these studies, researchers are only beginning to uncover the complex mechanisms by which epigenetic regulatory complexes function in the nervous system.

## 1.2 Epigenetics in intellectual disability

Intellectual disability (ID) is a common neurodevelopmental disorder, characterized by early onset limitations in both cognitive functioning and adaptive behaviour (American Psychiatric Association, 2013). Cognitive deficits are defined by an IQ of below 70, whereas limitations in adaptive behaviour correspond to deficits in an assortment of conceptual, social and practical skills (American Psychiatric Association, 2013). ID can be further subdivided into syndromic and non-syndromic forms. Patients diagnosed with syndromic forms of ID suffer from cognitive impairment, in addition to a wide variety of other clinical abnormalities (American Psychiatric Association, 2013). To date, more than 700 genes have been implicated in genetic forms of ID (Kochinke et al., 2016; Vissers et al., 2016). Studies in mice have revealed that many of these genes are required for neurogenesis, neuronal differentiation, neuronal migration and synaptogenesis in the developing brain (Vaillend et al., 2008). However, studies have found that a significant proportion of the mutated genes associated with ID encode for proteins involved in chromatin regulation (Kleefstra et al., 2014). For example, mutations in the *MECP2* gene have been implicated in Rett syndrome, an X-linked neurodevelopmental disorder characterized by ID and motor impairment (Amir et al., 1999). In addition, mutations in the euchromatin histone methyltransferase 1 (*EHMT1*) have been shown to cause Kleefstra syndrome (Mitra et al., 2017; Schwaibold et al., 2014). Furthermore, several components of the SWI/SNF chromatin remodelling complex are implicated in ID-related disorders such as Nicolaides-Baraitser syndrome and Coffin-Siris syndrome (Santen et al., 2012; Van Houdt et al., 2012).

Recent advances in next generation sequencing technology suggest that dominant *de novo* mutations are the most common cause of ID, especially severe forms (Gilissen et al., 2014; Vissers et al., 2010). In a recent study investigating the genetic causes of severe ID, dominant *de novo* copy number variations and single nucleotide variants were suggested to cause 60% of all cases, while rare inherited forms of ID only account for 2% (Gilissen et al., 2014). Currently, there are about 250 known dominant ID genes (Kochinke et al., 2016). Gene Ontology enrichment analysis performed in our lab has shown that these genes encode proteins that are highly enriched for processes involving chromatin regulation and gene transcription. In particular, the SWI/SNF chromatin remodelling complex is the most overrepresented protein complex among the known dominant ID genes (Figure 1). Eleven of the 29 genes that encode components of the human SWI/SNF complex have been implicated in ID, suggesting that this complex plays an important role in neuronal development or function (Di Donato et al., 2014; Dias et al., 2016; Hoyer et al., 2012; Johnston et al., 2013; Rivière et al., 2012; Santen et al., 2012; Santen et al., 2013; Tsurusaki et al., 2012; Van Houdt et al., 2012; Wieczorek et al., 2013; Wolff et al., 2012) (Figure 2).
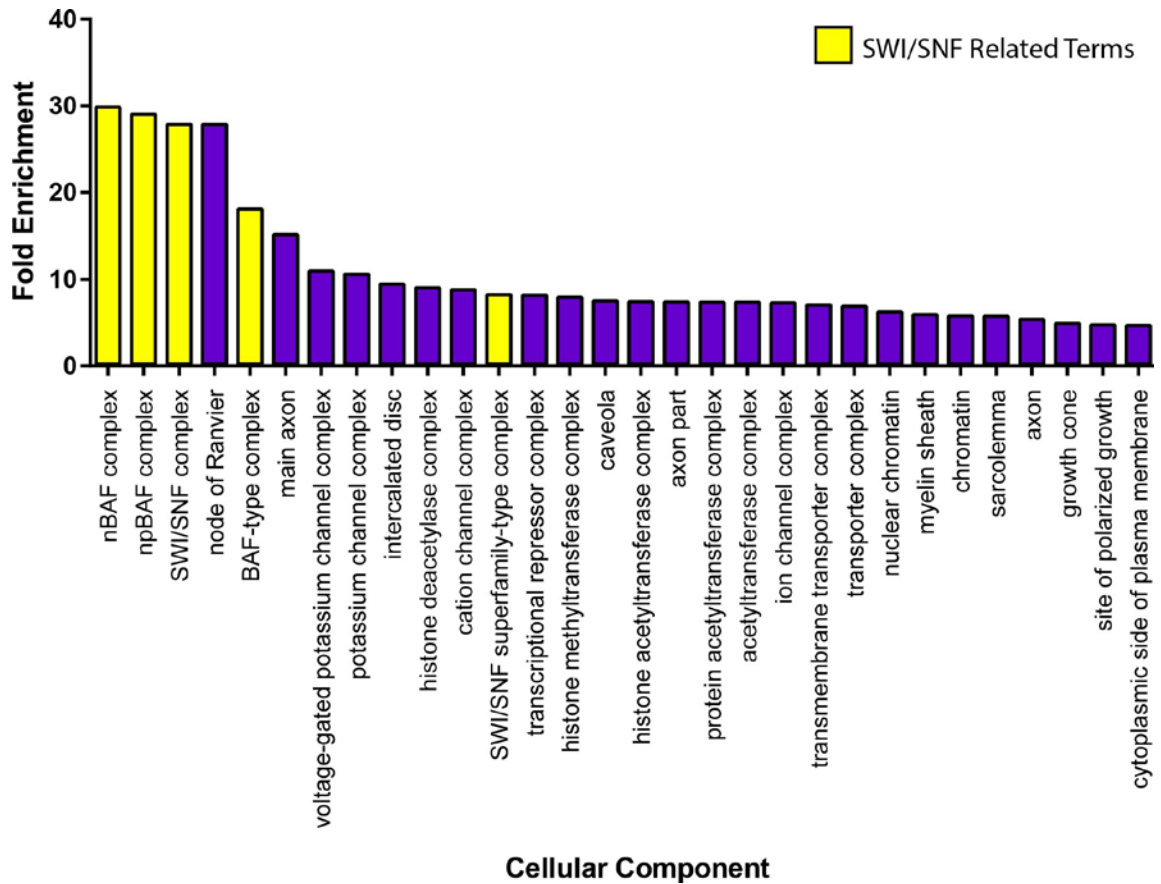
**Figure 1. The SWI/SNF complex is the most highly enriched cellular component among the dominant ID genes.**

Gene Ontology enrichment analysis (cellular components) was performed for the 291 dominant ID genes (http://sysid.cmbi.umcn.nl/). Bar plot shows the fold enrichment values for the top 30 most highly enriched cellular components. SWI/SNF related terms are highlighted in yellow.
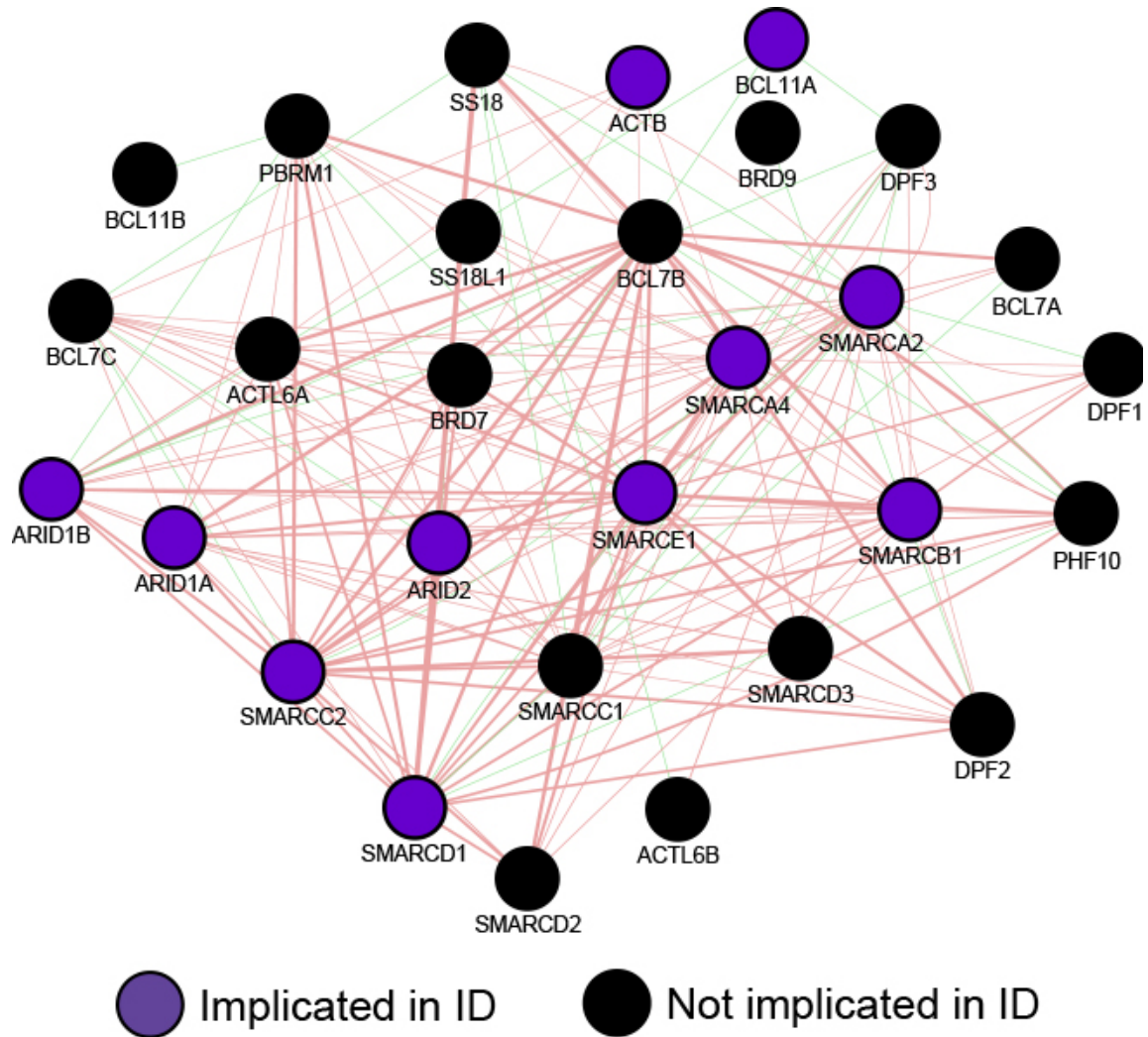
**Figure 2. Eleven of the 29 genes encoding components of the SWI/SNF complex have been implicated in ID.**

Protein-protein interaction network of the 29 human SWI/SNF complex proteins. The network was generated and visualized using the geneMANIA Cytoscape plug-in (v.3.5.0) (Franz et al., 2015). Genetic interactions are shown in blue and protein-protein interactions are shown in pink. Subunits highlighted in purple have been implicated in ID (Di Donato et al., 2014; Dias et al., 2016; Hoyer et al., 2012; Johnston et al., 2013; Rivière et al., 2012; Santen et al., 2012; Santen et al., 2013; Tsurusaki et al., 2012; Van Houdt et al., 2012; Wieczorek et al., 2013; Wolff et al., 2012).

## 1.3   SWI/SNF chromatin remodelling complex

The SWI/SNF complex is an ATP-dependent chromatin remodelling complex originally discovered in the yeast, *Saccharomyces cerevisiae*, due to its role in mating type switching and sucrose fermentation (Neigeborn & Carlson, 1984; Stern et al., 1984). The SWI/SNF complex is highly conserved, with homologous complexes identified in both mammals and *Drosophila* (Son & Crabtree, 2014) (Table 1). The SWI/SNF complex utilizes energy generated from the hydrolysis of ATP to slide, eject or restructure nucleosomes (Whitehouse et al., 1999). Studies have suggested a proposed mechanism through which the SWI/SNF complex remodels chromatin, often referred to as the DNA looping model. This model suggests that the ATPase functions as a DNA translocase, using the energy from ATP hydrolysis to force DNA around the nucleosome in the form of DNA waves. These movements disrupt the existing DNA-histone interactions, enabling movement of the nucleosome relative to the DNA (Havas et al., 2000; Zhang et al., 2006).

The mammalian SWI/SNF complex is referred to as the BAF (BRG1- or hBRM-associated factors) complex. The BAF complex consists of 15 subunits that are encoded by 29 genes from 15 gene families (Son & Crabtree, 2014). Ten of the 15 BAF subunits are encoded by multiple different genes from the same family (Lessard et al., 2007). Therefore, alternative subunits exist for multiple positions within the complex, enabling the BAF complex to undergo combinatorial assembly of its subunits (Kadoch & Crabtree, 2015). Each position within the BAF complex may be occupied by only one member of each protein family. For example, the BAF complex may contain one of two distinct ATPase subunits, Brahma (BRM) or Brahma-related gene 1 (BRG1) (Son & Crabtree, 2014). This feature has allowed for the assembly of highly specialized conformations that elicit cell-specific functions, including the embryonic stem cell (esBAF), neuronal progenitor (npBAF), and neuronal (nBAF) specific versions of the complex (Son & Crabtree, 2014).

In *Drosophila*, the SWI/SNF complex exists in two different forms, referred to as BAP (Brahma-associated protein) and PBAP (Polybromo-associated BAP) (Mohrmann et al., 2004). Both the BAP and PBAP complex contain the following core subunits: Bap55, Bap111, Act5C, Snr1, Moira (Mor), Bap60 and Brm (Mohrmann et al., 2004). However, each complex differs in the number and type of accessory protein subunits. The core SWI/SNF subunits associate with Osa to form the BAP complex, whereas the PBAP complex

is characterized by the absence of Osa, and the presence of E(y)3, Polybromo, and Bap170 (Chalkley et al., 2008; Mohrmann et al., 2004). In comparison to the mammalian BAF complex, the BAP complex contains 11 protein subunits. However, predictive software provided by the *Drosophila* RNAi Screening Center suggests that CG7154, CG10555, CG9650 and BCL7-like are orthologous to known members of the mammalian BAF complex (Hu et al., 2011). Although these proteins have yet to be verified as members of the SWI/SNF complex in *Drosophila*, their role in axon development of the *Drosophila* MB was studied in this project.

Genome-wide analysis of chromatin binding sites revealed that the BAP and PBAP versions of the complex target both distinct and overlapping regions of the genome, suggesting that certain genes may be solely regulated by either the BAP or PBAP version of the complex (Chalkley et al., 2008; Mohrmann et al., 2004). Both versions of the complex were shown to preferentially associate with regions of transcriptionally active chromatin, indicating that both the BAP and PBAP complexes share similar functions in transcriptional control (Moshkin et al., 2007). However, whole genome expression profiling revealed that only the BAP complex is involved in the regulation of cell cycle progression (Moshkin et al., 2007).

**Table 1. Evolutionary conservation of the SWI/SNF complex.**

| SWI/SNF (*S. cerevisiae*) | BAF/PBAF (*M.musculus*) | | BAP/PBAP (*D. melanogaster*) | |
|---|---|---|---|---|
| | BAF | PBAF | BAP | PBAP |
| Swi1p | Baf250a/Arid1a | | Osa | |
| Swi1p | Baf250b/Arid1b | | Osa | |
| | | Baf200/Arid2 | | Bap170 |
| Swi2p/Snf2p | Brm/Smarca2 | | Brm | |
| Swi2p/Snf2p | Brg1/Smarca4 | | Brm | |
| | | Baf180/Pbrm1 | | Polybromo |
| Swi3p | Baf155/Smarcc1 | | Mor | |
| | Baf170/Smarcc2 | | Mor | |
| | Baf100a/Bcl11a | | CG9650 | |
| | Baf100b/Bcl11b | | CG9650 | |
| Swp73p | Baf60a/Smarcd1 | | Bap60 | |
| | Baf60b/Smarcd2 | | Bap60 | |
| | Baf60c/Smarcd3 | | Bap60 | |
| | Baf57/Smarce1 | | Bap111 | |
| | Baf55a/Ss18 | | CG10555 | |
| | Baf55b/Crest/Ss18L | | CG10555 | |
| | B-actin/Actb | | Act5C | |
| Arp7p | Baf53a/Actl6a | | Bap55 | |
| Arp9p | Baf53b/Actl6b | | Bap55 | |
| Snf5p | Baf47/Smarcb1 | | Snr1 | |
| | Baf45a/Phf10 | | E(y)3/SAYP | |
| | Baf45b/Dpf1 | | D4 | |
| | Baf45c/Dpf2 | | D4 | |
| | Baf45d/Dpf3 | | D4 | |
| | Baf40a/Bcl7a | | BCL7-like | |
| | Baf40b/Bcl7b | | BCL7-like | |
| | Baf40c/Bcl7c | | BCL7-like | |
| | | Brd7 | CG7154 | |
| | Brd9 | | CG7154 | |
| Snf6p | | | | |
| Swp82p | | | | |
| Swp29p | | | | |

Adapted from Son & Crabtree (2014) and updated using the DIOPT ortholog prediction tool (v.6.0.1) (Hu et al., 2011). Subunits are organized into families and presented in the order of decreasing BAF protein size. Components of the mammalian SWI/SWI complex have been sorted into the BAF & PBAF specific subunits, whereas the components of the *Drosophila* complex have been sorted into BAP/PBAP specific subunits.

## 1.3.1    SWI/SNF complex in cellular differentiation and development

Several studies have implicated the SWI/SNF complex in processes related to cellular differentiation and development.  Studies in *Drosophila* have identified several components of the SWI/SNF complex that are required for the specification of segmental identity along the anteroposterior axis of the fly.  In particular, researchers identified Brm, Osa, Mor, Snr1, and E(y)3 as members of the trithorax group, a group of transcriptional activator proteins.  In *Drosophila*, these proteins function to maintain the appropriate expression of homeotic genes (Chalkley et al., 2008; Dingwall et al., 1995; Kennison & Tamkun, 1988).  In addition to being required for the organization of the insect body plan, the SWI/SNF complex is also involved in *Drosophila* tissue development.  Studies have shown that Brm, Snr1, and the BAP-specific subunit, Osa, are required for proper *Drosophila* wing development (Collins & Treisman, 2000; Herr et al., 2010; Zraly et al., 2003).  The Brm ATPase has been shown to regulate *Drosophila* wing development through the EGFR-Ras-MAPK signalling pathway (Herr et al., 2010), and the BAP-specific subunit Osa was found to disrupt the Wnt signalling pathway via repression of the wingless target genes, *decapentaplegic, Distal-less* and *nubbin* (Collins & Treisman, 2000).  In addition, null mutations in *Snr1* cause defects in wing vein development, including disruptions along the L2 vein and ectopic bristles on the L3 vein (Zraly et al., 2003).

The SWI/SNF complex has been shown to play an equally important role in mammalian development.  Studies have implicated the BAF complex in the differentiation of many different cell types, including adipocytes, hepatocytes, and erythropoietic cells (Romero & Sanchez-Cespedes, 2014).  Unlike the BAP complex found in *Drosophila*, the composition of the BAF complex varies according to cell type.  A specific conformation of the BAF complex is found in embryonic stem cells, referred to as esBAF.  This complex is defined by the presence of Baf155 and the ATPase Brg1, both of which appear to be required for the self-renewal and differentiation of embryonic stem cells (Ho et al., 2009).  In mice, knockdown of *Brg1* and *Baf155* resulted in early embryonic lethality due to impaired proliferation of the inner cell mass (Bultman et al., 2000; Kim et al., 2001).  A similar complex exists in neural stem cells, referred to as npBAF (Son & Crabtree, 2014).  Similar to the role of the esBAF complex, the npBAF complex has been shown to play a critical role in stem cell proliferation.  Mice containing heterozygous mutations in *Brg1* and *Baf155* had

defects in neural tube closure (Bultman et al., 2000; Kim et al., 2001). These findings demonstrate the importance of the SWI/SNF complex in development and exemplify the need to better understand the function of this conserved protein complex in the context of a whole organism.

## 1.3.2    Role of the SWI/SNF complex in neural development

The SWI/SNF complex is known to be important for cellular differentiation and tissue development (Romero & Sanchez-Cespedes, 2014). However, little is known about the role of this complex in the nervous system. Genetic screens in *Drosophila* have identified several components of the SWI/SNF complex that are important for the regulation of dendrite morphogenesis. In particular, one study found that knockdown of *brm*, *Bap55* and *Bap60* resulted in the misrouting of class I dendrite arborization (da) neurons (Parrish et al., 2006). Knockdown of *Bap55* also resulted in primary branch extension and a reduction in the dendritic arborization of class I da neurons, while knockdown of *Snr1* caused a reduction in lateral branching (Parrish et al., 2006). An additional screen in olfactory projection neurons revealed that *Bap55* is also required for dendrite targeting (Tea & Luo, 2011).

More recently, studies in mice have shown that the specific subunit composition of the SWI/SNF complex determines whether neural stem cells continue to divide or proliferate (Lessard et al., 2007; Yoo et al., 2009). As neural progenitors differentiate into post-mitotic neurons, the BAF complex undergoes subunit exchange. The npBAF-specific subunits Baf45a and Baf53a are replaced by Baf53b, Baf45b and Baf45c, members of the nBAF complex (Lessard et al., 2007; Olave et al., 2002). Notably, the SWI/SNF subunit, Baf53b, is exclusively expressed in post-mitotic neurons of the adult brain (Olave et al., 2002). A study in mice found that subdomain 2 of the neuron-specific subunit, Baf53b, is required for proper dendritic arborization, branching and synapse formation (Wu et al., 2007). *Baf53b* knockout mice had severe defects in activity-dependent dendritic outgrowth, synapse formation and axon myelination (Wu et al., 2007). These phenotypes were not rescued by overexpression of Baf53a, the npBAF-specific subunit. However, the observed defects in dendritic spine growth were successfully rescued upon replacement of the subdomain 2 region in Baf53a with the subdomain 2 region found in Baf53b (Wu et al., 2007). In accordance with this, mice deficient in Baf53b subdomain 2 exhibited defects in long term potentiation and

memory consolidation due to the disruption of actin polymerization at the synapse (Vogel-Ciernia et al., 2013). These deficits were found to result from the impaired phosphorylation of cofilin, a key regulator of actin polymerization (Vogel-Ciernia et al., 2017). Overall, these findings indicate that individual subunits of the SWI/SNF complex have important, yet distinct, functions in post-mitotic neurons.

## 1.4 *Drosophila* as a model for studies on neural development

*Drosophila melanogaster* is a species of fly belonging to the order Diptera and the family *Drosophilidae*. Often referred to as the common fruit fly, *Drosophila* has been used as a model organism in genetic research for over a century. The first documented use of *Drosophila* in the laboratory was by William Castle, a professor at Harvard University in 1901 (Castle, 1906). However, it was the unexpected discovery of the white-eyed mutation by T.H. Morgan in 1910 that initiated the widespread use of *Drosophila* in genetic research (Morgan, 1910). Building upon the work of Gregor Mendel, the discovery of the white mutation led to the establishment of sex-linked inheritance, prompting a revolution in our understanding of the physical basis of heredity. Prior to the 1950's, *Drosophila* were mainly used as a model organism to study genetics and heredity (Stephenson & Metcalfe, 2013). However, scientific advances have led to the development of a wide variety of important genetic tools, enabling key discoveries in neuroscience.

### 1.4.1 Advantages of *Drosophila* as a model organism

*Drosophila* offer an attractive model system for studying a wide range of biological processes, including heredity, embryogenesis, learning, behaviour and aging. As one of the first organisms to have its genome completely sequenced, *Drosophila* is one of the most well studied and understood eukaryotic model organisms. In comparison to the human genome, the genome of the fruit fly is significantly smaller, comprised of four chromosomes that encode roughly 120 million base pairs of DNA (Adams et al., 2000). Despite its small size, the *Drosophila* genome encodes approximately 17 000 protein coding genes (Gramates et al., 2017). Many of these genes have been conserved throughout evolution and are present in humans. In fact, comparison of the *Drosophila* and human genomes has shown that approximately 75% of human disease genes are conserved in *Drosophila* (Reiter et al., 2001).

In addition to the relatively high degree of genetic similarity between mammals and the fruit fly, *Drosophila* offer a number of practical advantages. *Drosophila* are relatively inexpensive and easy to maintain in large numbers. In comparison to other vertebrate systems, *Drosophila* are favoured due to their short generation time that takes place over a period of approximately ten days. In addition, female flies lay an average of 100 eggs per day (Jennings, 2011). These features facilitate genetic studies by enabling researchers to analyze large numbers of progeny over several generations within a matter of weeks. Finally, and perhaps most importantly, a wide variety of genetic tools have become available for use in *Drosophila* research. This has enabled researchers to study numerous different aspects of gene function at high resolution in specific cell populations.

## 1.4.2    Genetic tools available in *Drosophila*

The success of *Drosophila* as a model organism can largely be attributed to the development of a wide variety of sophisticated genetic tools and techniques. In genetic research, many studies are facilitated by the generation of mutant or transgenic flies. Transgenesis refers to the process of introducing foreign DNA, termed a transgene, into the genome of the host organism (Venken & Bellen, 2005). *P*-element mediated transformation was the first version of this technique to be developed, and remains one of the most common methods for transgene generation in *Drosophila.* *P*-elements are a type of class II transposable element found in the *Drosophila* genome (Castro & Carareto, 2004). The *P*-element encodes for transposase, an enzyme responsible for catalyzing both the excision and subsequent reinsertion of the *P*-element in the genome (Castro & Carareto, 2004). The natural *P*-element has been genetically modified to serve as a vector for germline transformation in *Drosophila*. Unlike the natural *P*-element, *P*-element mediated germline transformation requires that the transposase enzyme be transferred to a secondary plasmid known as the helper plasmid (Bachmann & Knust, 2008). In place of the transposase enzyme, a gene of interest is inserted into the plasmid containing the *P*-element. Each plasmid is then injected into the embryo at the posterior pole, the location at which the germline will be formed (Bachmann & Knust, 2008). Following cellularization, the transposase enzyme mediates transposition of the gene of interest into the DNA (Bachmann & Knust, 2008). Although useful in some aspects, *P*-elements are limited by their random integration behaviour. Moreover, *P*-elements are prone to position effects, as nearby

enhancers and silencers may affect the expression of the inserted transgene (Venken & Bellen, 2005). More recently, researchers have taken advantage of the phiC31 integrase (φC31) to enable site directed recombination between *attP* and *attB* recognition sites (Venken & Bellen, 2005). For use in *Drosophila*, *P*-element mediated transformation was used to generate a collection of lines with accurately mapped *attP* landing sites (Bischof et al., 2007). To mediate recombination, a plasmid containing both the transgene of interest and an *attB* recognition site are injected into the embryo, together with mRNA coding for the φC31 integrase (Fish et al., 2007). The *attP* site acts as a defined insertion site for plasmids containing the *attB* site, allowing for transgene insertion into known locations throughout the genome. Since the location of the *attP* sites can be precisely mapped, this technique minimizes the position effects associated with random *P*-element insertion.

The GAL4/UAS binary expression system is a powerful tool for the spatial and temporal control of gene expression in *Drosophila*. In this system, GAL4 is a transcriptional activator derived from yeast that activates the expression of genes under the control of the upstream activating sequence (UAS) (Brand & Perrimon, 1993). Each component of the UAS/GAL4 system is maintained in separate lines, commonly referred to as the driver and responder. Genes placed under the control of the UAS enhancer are only transcribed in the presence of the GAL4 transcription factor (Duffy, 2002). As a result, transcription of the target gene will only be activated when the driver and responder lines are crossed together (Figure 3). Depending on the promoter used to drive GAL4 expression, the target gene may be expressed in a specific tissue, at a specific time point, or ubiquitously. Thousands of GAL4 lines are currently available from public stock centers, each expressing GAL4 in a distinct pattern throughout development. This has greatly facilitated studies in the field of *Drosophila* neurobiology by allowing researchers to follow and manipulate distinct neuronal subsets in the fly brain (Jenett et al., 2012).
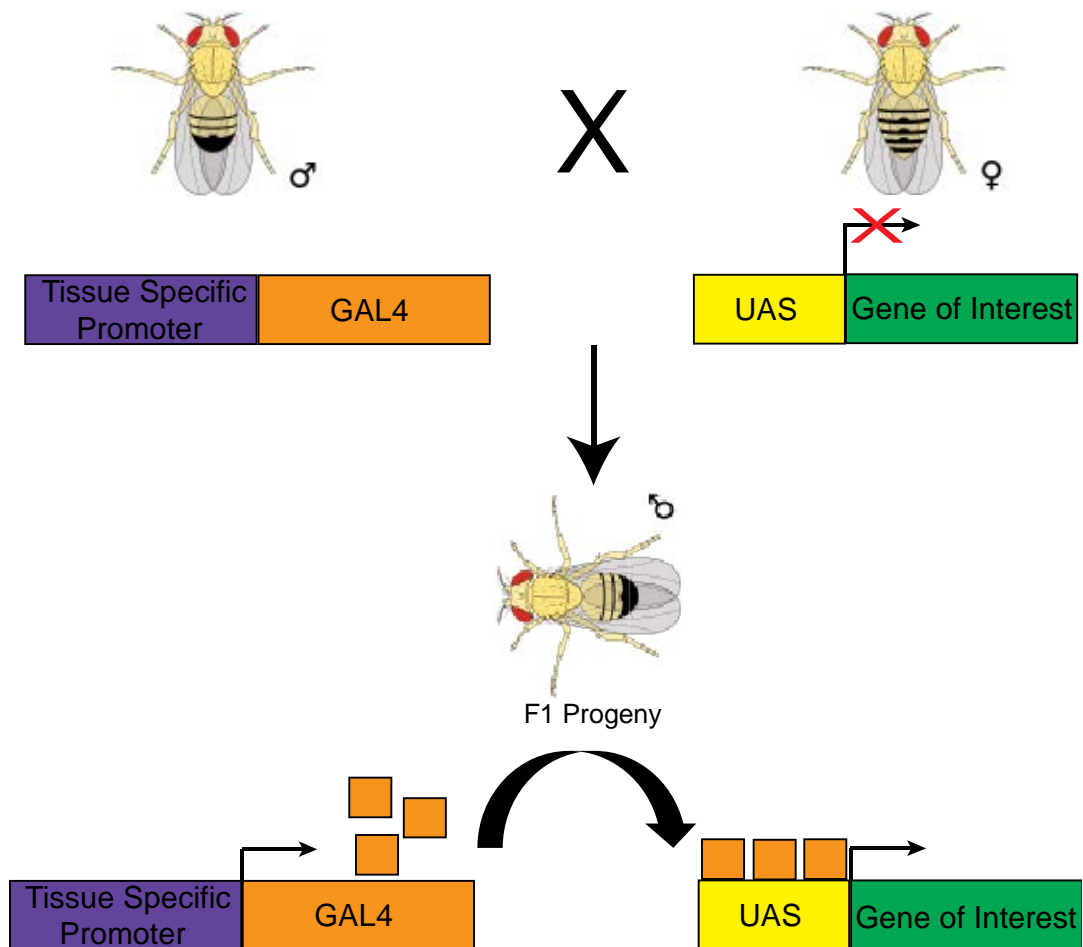
**Figure 3. The GAL4/UAS system allows for the tissue-specific manipulation of gene expression.**

Flies carrying the GAL4 transcription factor under the control of a tissue-specific promoter are mated with flies carrying a gene of interest under the control of the UAS. Both elements will be present in the progeny of the cross, enabling for GAL4/UAS binding and expression of the gene of interest in a tissue-specific manner.

Another beneficial way to study gene function is via the post transcriptional silencing of gene expression. This can be accomplished through the use of inducible RNA interference (RNAi) technology. RNAi is a biological process in which double stranded RNA (dsRNA) molecules are used to direct sequence-specific gene silencing (Giordano et al., 2002). Initially discovered in *Caenorhabditis elegans* (Fire et al., 1998), RNAi has become an extremely valuable research tool in *Drosophila* for the study of gene function. The RNAi pathway is initiated by the enzyme, Dicer-2, which cleaves long dsRNA molecules into smaller fragments of short interfering RNA (siRNA). Following cleavage, siRNA molecules are integrated into the RNA induced silencing complex (RISC) and used to direct sequence specific degradation of the target mRNA, resulting in reduced protein (Giordano et al., 2002) (Figure 4). Thousands of RNAi stocks are currently available from public stock centers (Dietzl et al., 2007), allowing for researchers to carry out large genetic screens. Furthermore, RNAi technology can be used in combination with the UAS/GAL4 system for targeted gene knockdown in a cell or tissue-specific manner.
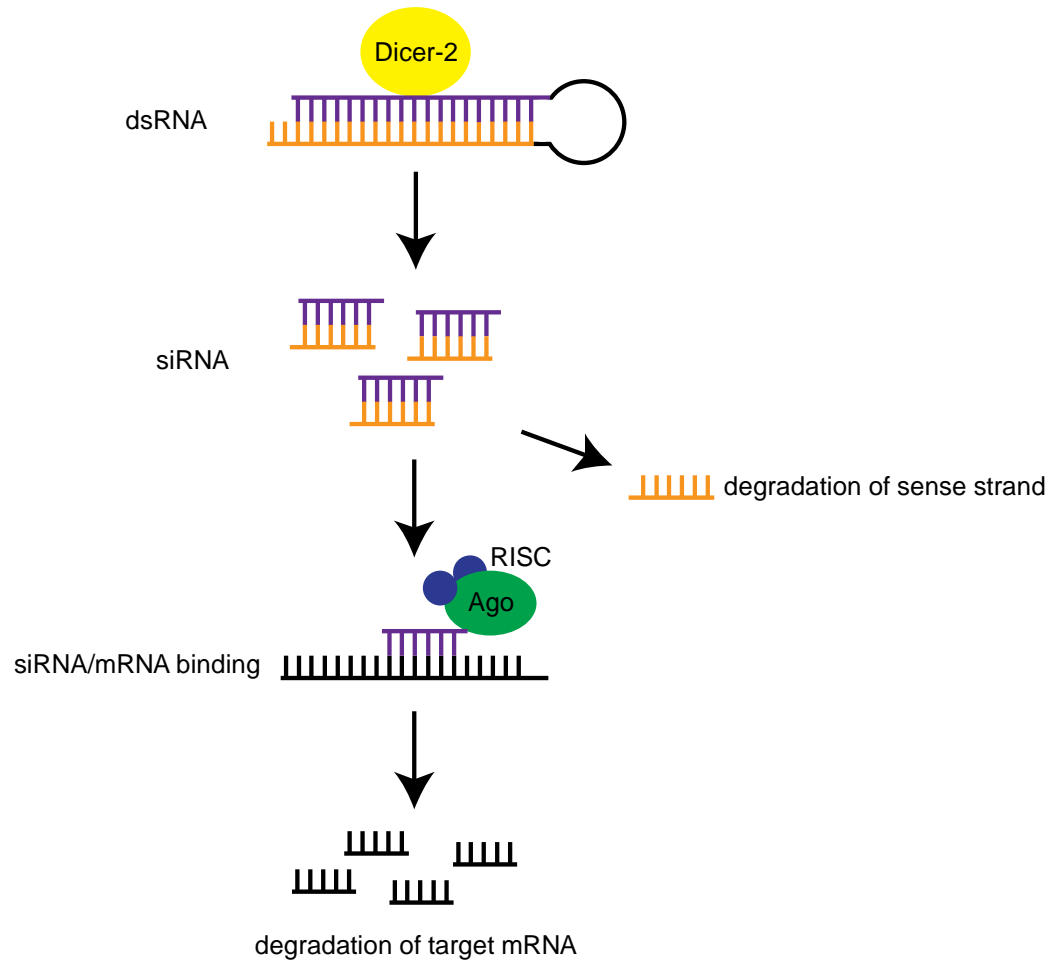
**Figure 4. RNAi is an effective method for the knockdown of gene expression in *Drosophila*.**

The RNAi pathway is initiated by the Dicer-2 enzyme, which cleaves long dsRNA molecules into siRNA. The antisense strand of the siRNA molecule is loaded into the RISC complex to enable complementary binding of the siRNA to the target mRNA.

## 1.5   Development of the *Drosophila* mushroom body

MB's are symmetrically paired neuropil structures in the brain of *Drosophila*, each containing a dense network of axons, dendrites and glial cell processes (Heisenberg, 1998). MB's receive olfactory information from the antennal lobe through MB projection neurons (Aso et al., 2014; Lee et al., 1999).  In accordance with this, behavioural studies have shown that the *Drosophila* MB's are required for olfactory learning and memory (Davis, 1996; Heisenberg, 1998).  MB neurons are derived from Kenyon cells (Kurusu et al., 2002).  Each Kenyon cell projects dendrites into the calyx and axons into the central brain, where they form the α, β, α', β' and γ-lobes (Lee et al., 1999).  In the adult brain, each MB is composed of approximately 2000 neurons that arise from the division of four distinct neuroblast cells (Aso et al., 2014; Lee et al., 1999).   MB neuroblasts divide continuously throughout development, giving rise to three distinct classes of MB neurons (α/β, α'/β' and γ) in a sequential fashion (Kurusu et al., 2002; Lee et al., 1999) (Figure 5).  The proper development of the MB is dependent on a neuronal remodelling process that involves axon guidance and pruning.  The γ neurons are the first to arise, projecting their axons into both the dorsal and medial lobes during the late embryonic and early larval stages of development (Lee et al., 1999).  This is followed by the generation of the α′/β′ neurons during the late larval stage and the α/β neurons during the pupal stage of development (Lee et al., 1999).  Shortly after puparium formation, γ neurons undergo an extensive remodelling process in which axon pruning reduces the larval specific γ axons back to the peduncle (Lee et al., 1999).  During the pupal stage of development, adult γ neurons only re-extend their axons into the medial lobe (Lee et al., 1999).  The development of the *Drosophila* MB's has been well described and the axonal projections are easily visualized.  Consequently, they are a useful model for studying various aspects of axon development including general axon guidance and neuronal remodelling.
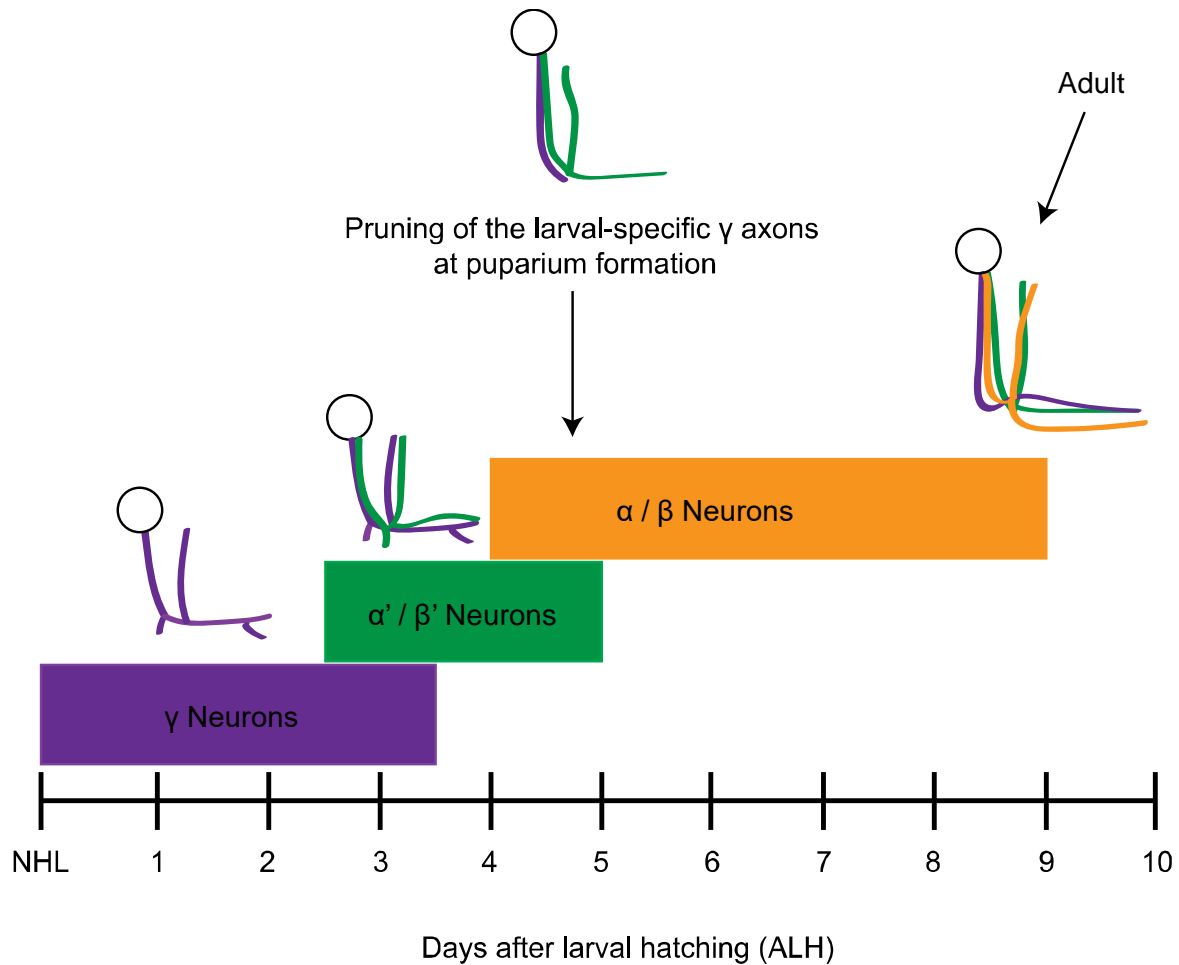
**Figure 3. Sequential development of the *Drosophila* mushroom body.**

The *Drosophila* MB is composed of three distinct classes of neurons (α/β, α'/β' and γ) that are generated in a specific temporal order throughout development. The γ neurons are the first to arise in newly hatched larvae (NHL), extending axons into both the dorsal and medial lobes of the MB. During puparium formation, axon pruning reduces the larval specific γ axons back to the peduncle. During pupal development, the γ neurons re-extend their axons into the medial lobe. The generation of the different types of MB neurons has completed by approximately 9 days after larval hatching (ALH). Adapted from (Lee et al., 1999).

Several studies have implicated the insect steroid hormone, ecdysone, and the ecdysone hormone receptor in the neuronal remodelling of the *Drosophila* MB (Lee et al., 2000; Schubiger et al., 1998). In *Drosophila*, the functional ecdysone receptor is formed by the interaction of the Ecdysone receptor protein (EcR) and the Ultraspiracle protein (USP) (Yao et al., 1993). To induce neuronal remodelling, ecdysone must bind the EcR/USP nuclear receptor (Lee et al., 2000). In accordance with this, MB γ neurons containing a homozygous loss of function mutation in *usp* failed to prune (Lee et al., 2000). There are three different EcR isoforms, referred to as EcR-A, EcR-B1 and EcR-B2 (Schubiger et al., 1998). The expression of the various EcR isoforms is differentially regulated in different cell types of the *Drosophila* MB (Schubiger et al., 1998). Notably, EcR-B1 is highly and specifically expressed in the MB γ neurons prior to puparium formation (Schubiger et al., 1998). Loss of function mutations in *EcR-B1* also result in defective γ pruning, demonstrating the importance of the EcR/USP receptor in γ-neuron remodelling (Lee et al., 2000). The expression of the EcR-B1 isoform is tightly regulated by the TGF-β signalling pathway (Zheng et al., 2003). TGF-β signalling is initiated by the binding of myoglianin to the TGF-β type I receptor, baboon, and either one of the TGF-β type II receptors; punt or wishful thinking (Awasaki & Lee, 2011; Zheng et al., 2003). Binding of myoglianin to the baboon receptor leads to phosphorylation of Smad on X, a protein that acts downstream to regulate the expression of genes that in turn upregulate the expression of EcR-B1 (Zheng et al., 2003). However, the target genes responsible for the upregulation of EcR-B1 expression have yet to be identified. In a separate study, Boulanger and colleagues found that the Ftz-f1 nuclear receptor is required for remodelling of the MB γ neurons. Ftz-f1 activation leads to the upregulation of the EcR-B1 isoform and repression of *Hr39*, an *ftz-f1* paralog known to inhibit axon pruning in the γ neurons (Boulanger et al., 2011). This mechanism was found to act independently of TGF-β signalling, suggesting that multiple different pathways converge to regulate EcR-B1 expression and ensure proper neuronal remodelling. A recent study has also suggested the involvement of the non-coding RNA molecule, microRNA-34 (miR-34). Ectopic over expression of miR-34 in differentiated MB γ neurons was found to impair γ axon pruning through downregulation of the EcR-B1 receptor (Lai et al., 2016). This phenotype was rescued through overexpression of either the EcR-B1 isoform or the baboon receptor, suggesting that miR-34 may be involved in the regulation of EcR-B1 expression through the TGF-β signalling pathway (Lai et al., 2016). Overall, these findings suggest that

axon pruning of the MB γ neurons may be dependent on the epigenetic regulation of multiple parallel pathways which converge to regulate the expression of the EcR-B1 receptor.

## 1.6 Research hypothesis and rationale

ID is a complex and highly heterogeneous disorder affecting 1-3% of the global population (Harris, 2006). Affected individuals suffer lifelong impairments in cognitive function and adaptive behaviour, placing a significant burden on family members and the healthcare system. Despite the large number of known ID genes, the specific mechanisms underlying the aetiology of ID are not fully known. However, analysis of the known ID genes has revealed that defects in chromatin regulation represent one of the most common causes underlying ID (van Bokhoven & Kramer, 2010). As previously mentioned, the SWI/SNF chromatin remodelling complex is one of the most statistically overrepresented protein complexes involved in the aetiology of ID (30.06-fold enrichment of the nBAF complex). Studies have implicated several members of the SWI/SNF complex in a number of ID-related disorders, including Autism Spectrum disorder, Coffin-Siris syndrome and Kleefstra syndrome (Di Donato et al., 2014; Dias et al., 2016; Rivière et al., 2012; Santen et al., 2012; Santen et al., 2013; Tsurusaki et al., 2012; Van Houdt et al., 2012; Wolff et al., 2012). Despite the important role of the SWI/SNF complex in neurodevelopmental disorders, little is known about the function of this complex in the nervous system. Studies have investigated the role of this complex in the regulation of dendrite morphology, but the mechanisms underlying the observed defects in dendrite morphology remain unknown (Tea & Luo, 2011; Wu et al., 2007). Furthermore, the role of the SWI/SNF complex in axon development has yet to be explored. Lastly, the role of this complex in the development of brain regions important for learning and memory is unknown. The aim of this research is to systematically characterize the role of the SWI/SNF chromatin remodelling complex in the post-mitotic axonal development of the *Drosophila* MB. I hypothesize that SWI/SNF mediated gene regulation plays an important role in post-mitotic neuronal development and I predict that MB-specific knockdown of the SWI/SNF components will result in morphological defects that result from altered axon guidance or neuronal remodelling. To test this hypothesis, I have accomplished two key objectives:

1) Identify and classify gross morphological defects in MB development following RNAi-mediated gene knockdown of all 15 individual SWI/SNF subunits.

2) To determine whether the observed defects in gross MB morphology result from defects in axon guidance or neuronal remodelling.

This study will lay the foundation for future studies aimed at understanding the molecular mechanisms disrupted in the MB upon SWI/SNF knockdown.

# Chapter 2

## 2 METHODS

## 2.1 Fly stocks and culture

All fly stocks were maintained at room temperature on standard cornmeal-agar media. All of the fly strains used in this study were obtained from either the Bloomington *Drosophila* Stock Center (BDSC) (Bloomington, USA) or the Vienna *Drosophila* Resource Center (VDRC) (Vienna, Austria), with the exception of *MB607B-GAL4* which was obtained from the Janelia Fly light collection (Ashburn, USA) (Appendix A). The inducible RNAi stocks obtained from the BDSC were generated by the Transgenic RNAi Project (TRiP) via φC31 mediated site-specific recombination (Perkins et al., 2015). Transgenic RNAi stocks generated by the TRiP utilize five different vectors for hairpin insertion, namely the VALIUM1, VALIUM10, VALIUM20, VALIUM21, and VALIUM22 vectors. Lines generated using the VALIUM20, VALIUM21, and VALIUM22 vectors utilize short hairpin RNA molecules (Ni et al., 2011), whereas lines generated using the VALIUM1 and VALIUM10 vectors use long hairpin RNA molecules (Ni et al., 2008; Ni et al., 2009). The VDRC lines used in this study were obtained from two different genetic libraries, each of which uses a different method for hairpin insertion. Similar to the lines generated by the TRiP, stocks obtained from the KK library of the VDRC were generated using φC31 mediated site-directed recombination (Green et al., 2014). Conversely, lines obtained from the GD library were generated using *P*-element mediated germ line transformation (Dietzl et al., 2007).

For all knockdown experiments, controls were generated using the appropriate genetic background stocks (Appendix B). All of the stocks obtained from the VALIUM1, VALIUM10, VALIUM21, and VALIUM22 collections of the TRiP contain a transgene on the third chromosome, whereas stocks obtained from the VALIUM20 collection include a combination of second and third chromosome transgenes. To account for the third chromosome based transgenes, genetic control animals were generated using the *attP2* (third chromosome) genetic background control strain (genotype: [$y^1v^1$; *P{CaryP}attP2*]) and a hairpin stock targeting mCherry (genotype: [$y^1sc^*v^1$; *P{VALIUM20-mCherry}attP2*]). Both the *attP2* genetic background stock and the mCherry control have the same genetic

background as the third chromosome based transgenes obtained from the TRiP. However, the mCherry control also contains an RNAi construct targeting the fluorophore mCherry, a protein that does not exist in the *Drosophila* genome (Perkins et al., 2015). Due to the presence of the non targeting RNAi, the hairpin stock targeting mCherry is more similar to the RNAi lines used in this study than that of the *attP2* background stock. Therefore, statistical analyses were performed by comparing the third chromosome based transgenes to the mCherry-RNAi hairpin control instead of the *attP2* genetic background stock. VALIUM20 stocks containing a transgene on the second chromosome were compared to the *attP40* (second chromosome) genetic background control strain (genotype: $[y^1v^1;$ *P{CaryP}attP40*]). Finally, the isogenic host strain, $[w^{1118}]$, was used as a genetic background control for the GD library, whereas the genetic background stock, $[yw^{1118};P\{attP,y^+,w^3\}]$, was used as a control for the KK library.

## 2.2  Genetic crosses

All crosses were performed at 29°C in 70% humidity on a 12h-12h light-dark cycle. Individual SWI/SNF subunits were knocked down in the MB using targeted RNAi in combination with the UAS-GAL4 binary expression system. MB-specific knockdown was achieved using the *R14H06-GAL4* transgene, which specifically expresses GAL4 in post-mitotic MB cells (Jenett et al., 2012). For visualization of the MB, *R14H06-GAL4* was combined with *UAS-mCD8::GFP* using standard genetic techniques. The RNAi constructs used in this study consist of both short and long hairpin RNA molecules. Dicer-1 is endogenously expressed in the fly, and this expression has proven to be effective for the processing of short hairpin RNAs (Ni et al., 2011; Perkins et al., 2015) (TRiP's VALIUM20, VALIUM21 & VALIUM22 collections). However, it has been shown that long hairpins require the co-expression of Dicer-2 to achieve optimal knockdown (Dietzl et al., 2007) (TRiP's VALIUM1 & VALIUM10 collections, VDRC's GD & KK libraries). Therefore, *UAS-Dicer-2* was co-expressed in the MB when long hairpin RNA lines were used for knockdown. For knockdown experiments, males from short hairpin RNA lines were crossed to females of the genotype $[w^{1118};$ *P{UAS-mCD8::GFP.L}LL5, P{UAS-mCD8::GFP.L}2)/CyO; P{GMR14H06-GAL4}attP2)/TM6*], whereas males from long hairpin RNAi lines were crossed to females of the genotype $[w^{1118};$ *P{UAS-Dcr-2.D}2/CyO; P{GMR14H06-GAL4}attP2), P{UAS-mCD8::GFP.L}LL6/TM6*]. Parents were removed

prior to eclosion and adult males of the appropriate genotype were collected from the F1 knockdown progeny for dissection (Table 2). To account for potential off target effects, MB-specific knockdown of the SWI/SNF genes was performed using at least two different RNAi constructs that target different regions of the endogenous mRNA.

Defects in γ-neuron remodelling were investigated using the *MB607B-GAL4* driver, which has been shown to specifically express GAL4 in a small subset of the MB γ neurons (Aso et al., 2014). Remodelling defects were investigated for the SWI/SNF genes *Bap60*, *Snr1* and *e(y)3*. For visualization of the MB γ neurons, RNAi constructs were combined with *UAS-mCD8::GFP* using standard genetic techniques. To visualize the adult specific projection patterns of the MB γ neurons, females of the genotype [$w^{1118}$; *P{UAS-mCD8::GFP}/CyO; P{UAS-RNAi}/TM6*] were crossed to males collected from the *MB607B-GAL4* driver (genotype: [*R19B03-p65ADZp; R39A11-39A11_ZpGAL4DBD*]). Newly eclosed males of the genotype [$w^{1118}$; *P{UAS-mCD8::GFP}/R19B03-p65ADZp}; P{UAS-RNAi}/{R39A11-39A11_ZpGAL4DBD}*] were collected for dissection and compared to flies of the control genotype [$w^{1118}$;*P{UAS-mCD8::GFP}/R19B03-p65ADZp};P{VALIUM20-mCherry}attP2}/ {R39A11-39A11_ZpGAL4DBD}*].

**Table 2. Genotypes of the control and knockdown flies analyzed for defects in gross MB morphology.**

| | Control Genotypes | Knockdown Genotypes |
|---|---|---|
| attP2 VALIUM20/21/22 | $\frac{w^{1118}}{Y}$ ; $\frac{UAS\text{-}mCD8::GFP}{+}$ ; $\frac{R14H06\text{-}GAL4}{attP2}$ | $\frac{w^{1118}}{Y}$ ; $\frac{UAS\text{-}mCD8::GFP}{+}$ ; $\frac{R14H06\text{-}GAL4}{UAS\text{-}RNAi}$ |
| attP2 (Dcr-2) VALIUM1/10 | $\frac{w^{1118}}{Y}$ ; $\frac{UAS\text{-}Dcr2}{+}$ ; $\frac{R14H06\text{-}GAL4,\ UAS\text{-}mCD8::GFP}{attP2}$ | $\frac{w^{1118}}{Y}$ ; $\frac{UAS\text{-}Dcr2}{+}$ ; $\frac{R14H06\text{-}GAL4,\ UAS\text{-}mCD8::GFP}{UAS\text{-}RNAi}$ |
| mCherry VALIUM20/21/22 | $\frac{w^{1118}}{Y}$ ; $\frac{UAS\text{-}mCD8::GFP}{+}$ ; $\frac{R14H06\text{-}GAL4}{UAS\text{-}mCherry}$ | $\frac{w^{1118}}{Y}$ ; $\frac{UAS\text{-}mCD8::GFP}{+}$ ; $\frac{R14H06\text{-}GAL4}{UAS\text{-}RNAi}$ |
| mCherry (Dcr-2) VALIUM1/10 | $\frac{w^{1118}}{Y}$ ; $\frac{UAS\text{-}Dcr2}{+}$ ; $\frac{R14H06\text{-}GAL4,\ UAS\text{-}mCD8::GFP}{UAS\text{-}mCherry}$ | $\frac{w^{1118}}{Y}$ ; $\frac{UAS\text{-}Dcr2}{+}$ ; $\frac{R14H06\text{-}GAL4,\ UAS\text{-}mCD8::GFP}{UAS\text{-}RNAi}$ |
| attP40 | $\frac{w^{1118}}{Y}$ ; $\frac{UAS\text{-}mCD8::GFP}{attP40}$ ; $\frac{R14H06\text{-}GAL4}{+}$ | $\frac{w^{1118}}{Y}$ ; $\frac{UAS\text{-}mCD8::GFP}{UAS\text{-}RNAi}$ ; $\frac{R14H06\text{-}GAL4}{+}$ |
| GD (Chromosome 2) | $\frac{w^{1118}}{Y}$ ; $\frac{UAS\text{-}Dcr2}{+}$ ; $\frac{R14H06\text{-}GAL4,\ UAS\text{-}mCD8::GFP}{+}$ | $\frac{w^{1118}}{Y}$ ; $\frac{UAS\text{-}Dcr2}{UAS\text{-}RNAi}$ ; $\frac{R14H06\text{-}GAL4,\ UAS\text{-}mCD8::GFP}{+}$ |
| GD (Chromosome 3) | $\frac{w^{1118}}{Y}$ ; $\frac{UAS\text{-}Dcr2}{+}$ ; $\frac{R14H06\text{-}GAL4,\ UAS\text{-}mCD8::GFP}{+}$ | $\frac{w^{1118}}{Y}$ ; $\frac{UAS\text{-}Dcr2}{+}$ ; $\frac{R14H06\text{-}GAL4,\ UAS\text{-}mCD8::GFP}{UAS\text{-}RNAi}$ |
| KK | $\frac{w^{1118}}{Y}$ ; $\frac{UAS\text{-}Dcr2}{attP,y[+],w[3']]}$ ; $\frac{R14H06\text{-}GAL4,\ UAS\text{-}mCD8::GFP}{+}$ | $\frac{w^{1118}}{Y}$ ; $\frac{UAS\text{-}Dcr2}{UAS\text{-}RNAi}$ ; $\frac{R14H06\text{-}GAL4,\ UAS\text{-}mCD8::GFP}{+}$ |

Adult males of the above genotypes were collected for dissection. Third chromosome based transgenes obtained from the TRiP include a combination of short (VALIUM1, VALIUM10) and long hairpin RNA molecules (VALIUM20, VALIUM21, VALIUM22). RNA stocks generated using the VALIUM1 and VALIUM10 vectors of the TRiP were co-expressed with *UAS-Dicer-2*.

## 2.3   Adult brain dissection and confocal microscopy

The brains of adult males were dissected in phosphate buffered saline (pH 7.2) and fixed with 4% paraformaldehyde for 45 minutes at room temperature. Brains were mounted in Vectashield (Vector Laboratories) and imaged using a Zeiss LSM 510 duo vario confocal microscope. Confocal stacks were generated using 100 µm slices and processed using Image J software (Fiji) (Schindelin et al., 2012) and Adobe Photoshop.

## 2.4   Lethality assay

To determine which of the RNAi lines used in this study resulted in lethality upon ubiquitous knockdown, *Actin5C-GAL4* was used to induce ubiquitous SWI/SNF expression. Female flies heterozygous for *Actin5C-GAL4 (*genotype: [$y^1w^*$; *P{Act5C-GAL4-w}E1/CyO*]) were crossed with male responder flies containing a *UAS-RNAi* transgene specific to one of the 15 SWI/SNF subunits. Three biological replicates were performed for each SWI/SNF subunit at 25ºC in 70% humidity on a 12h-12h light-dark cycle. The *Actin5C-GAL4* transgene is balanced over the CyO balancer chromosome. As a result, 50% of the progeny are expected to receive the *Actin5C-GAL4* transgene, whereas the remaining 50% are expected to receive the CyO balancer chromosome which contains a dominant marker mutation for curly wings. F1 progeny were scored for the presence or absence of the curly wing marker. The proportion of straight winged flies indicated survival with *Actin5C-GAL4* driven expression of RNAi constructs. Percent survival was calculated by comparing the number of flies with straight wings to the number of flies with curly wings ($\% Survival = \frac{Nstraig\ htwingprogeny}{Ncurlywingprogeny}$). Deviations from expected frequencies were calculated using a Chi-square statistical test.

## 2.5   Scoring and classification of mushroom body phenotypes

Gross MB morphology was assessed by examining the individual slices (z= 1.0 µm) of brains with *R14H06*-directed GFP-expression. Due to the high degree of natural variation in the size of the *Drosophila* MB, confocal stacks were qualitatively assessed for defects in MB morphology. Four distinct phenotypes were observed, including the appearance of missing α and β lobes, β-lobe fibers crossing over the midline, extra dorsal projections and

stunted γ-lobes. As previously mentioned, the adult MB is a symmetrically lobed structure in the brain of *Drosophila*. In some cases, knockdown resulted in loss of both the right and left α/β lobes. To simplify the analysis, the missing lobe phenotype was scored on a presence or absence basis, regardless of the number of lobes missing. The remaining three phenotypes were quite variable in severity. As a result, each brain was classified as 'normal', 'mild', 'moderate', or 'severe'. The β-lobe crossing phenotype was scored based on the width and density of GFP labelled β-lobe fibers crossing the midline. In most cases, this phenotype was bilaterally symmetric. However, in some cases, the β-lobe fibers appeared to extend from only one side of the MB. Regardless of whether the β-lobe crossing phenotype was bilateral or unilateral, phenotype severity was scored according to the same criteria stated above. The extra dorsal projection phenotype was classified based on the number and thickness of dorsal projections adjacent to the α-lobe, whereas the stunted γ-lobe phenotype was classified based on the relative size of the γ-lobe.

## 2.6  Quantification of fluorescent signal intensity

Image J software (Fiji) (Schindelin et al., 2012) was used to quantify the difference in fluorescent signal intensity between the α and γ-lobes of the *Drosophila* MB. The multipoint selection tool was used to sample four defined regions within each of the MB α and γ-lobes (Figure 6). The average gray value within each selection was calculated in order to determine the intensity of GFP expression at each of the defined points within the α and γ-lobes. Fluorescent signal ratios were calculated for each side of the MB according to the following formula:

$$Fluorescent\ Signal\ Intensity\ Ratio = \frac{\sum \gamma^{(1-4)}}{\sum \alpha^{(1-4)}}$$

A global average ratio was calculated for each image by taking the average of the left and right MB ratios. Brightness ratios were calculated for each individual image and an average was calculated for each genotype.
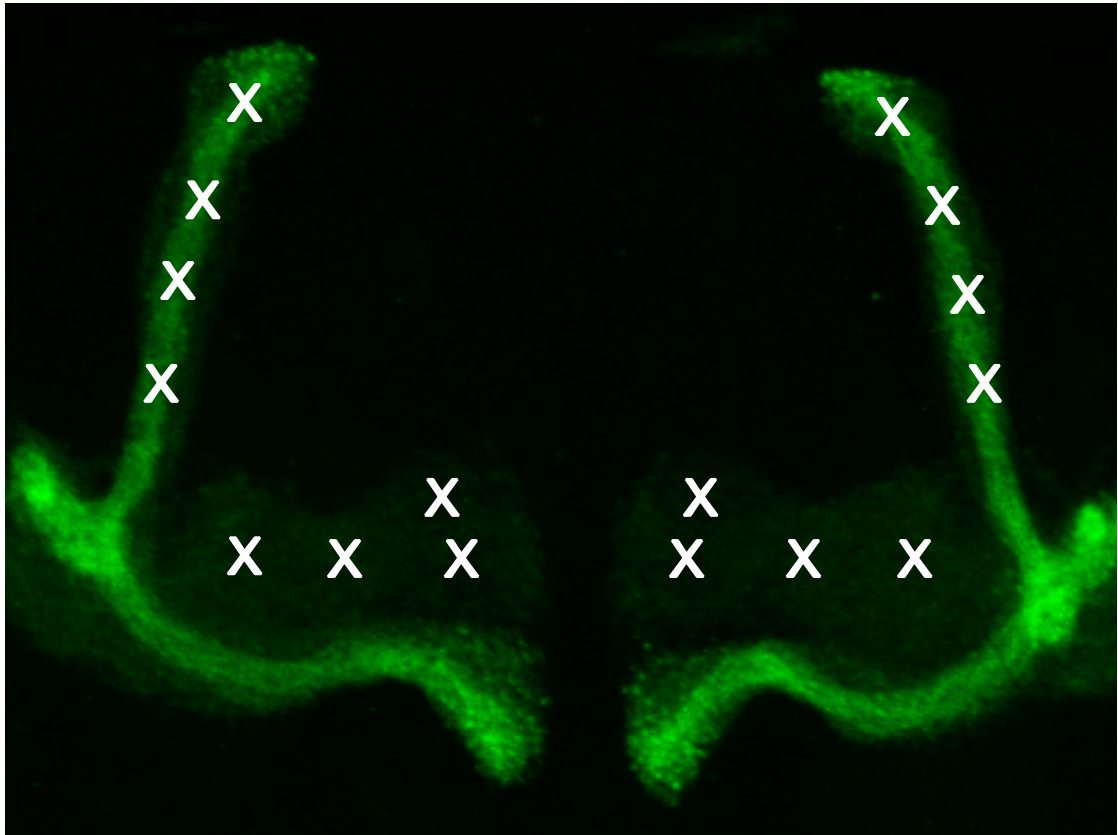
**Figure 6. Representation of the locations in which the fluorescent signal of the mushroom body was measured.**

Fluorescent signal intensity was measured at four distinct points within each of the MB α and γ-lobes. The approximate location in which each measurement was taken is marked by an X.

## 2.7   Statistical analysis of mushroom body phenotypes

SWI/SNF knockdown resulted in an apparent increase in the frequency of extra dorsal projections, stunted γ-lobes and β-lobe fibers crossing the midline.  For each of these phenotypes, the proportion of MB's exhibiting abnormal morphology (sum of mild, moderate and severe proportions) was compared to the proportion exhibiting normal morphology between each knockdown and the appropriate control using a two-tailed Fisher's exact test. The Bonferroni-Dunn test was used as a follow up to correct for multiple comparisons.

To determine whether there was a significant reduction in the relative γ-lobe intensity of SWI/SNF knockdown flies, the relative signal intensity of knockdown flies was compared to that of the mCherry-RNAi hairpin control using a one-way ANOVA with Dunnet's test for multiple comparisons.

# Chapter 3

# 3    RESULTS

## 3.1    Survival of *Actin5C-GAL4* mediated SWI/SNF knockdown

Null mutations in several components of the SWI/SNF complex have been shown to cause embryonic lethality (Bultman et al., 2000; Klochendler-Yeivin et al., 2000). Therefore, it was expected that ubiquitous knockdown of the SWI/SNF subunits would result in lethality. To determine which RNA lines caused lethality upon ubiquitous knockdown, we used *Actin5C-GAL4* to induce RNAi expression in all cells.

Ubiquitous knockdown caused a significant reduction in percent survival as compared to expected values for 26 of the 31 RNAi lines tested (Table 3). A complete or almost complete reduction in survival was observed for 22 RNAi lines (% survival ≤ 5.00, P<1x10$^{-4}$), whereas a partial reduction in survival was observed following knockdown of *UAS-Snr1[12644]* (% survival= 53.8 ± 18.8, P= 0.010), *UAS-BCL7-like[20410]* (% survival= 43.6 ± 5.78, P<1x10$^{-4}$), *UAS-Act5C[42651]* (% survival= 31.4 ± 36.2, P= 5.8x10$^{-3}$), and *UAS-Bap60[33954]* (% survival= 17.8 ± 12.4, P<1x10$^{-4}$). Conversely, knockdown of *UAS-BCL7-like[35714]* (% survival= 96.9 ± 13.2, P= 0.983), *UAS-CG10555[50606]* (% survival= 98.0 ± 37.4, P= 0.998), *UAS-Bap55[31708]* (% survival= 83.3 ± 23.3, P= 0.884), *UAS-brm[34520]* (% survival= 77.8 ± 15.6, P= 0.137) and *UAS-polybromo[32840]* (% survival= 102 ± 12.2, P= 0.482) caused no significant reduction in percent survival as compared to expected population frequencies. However, Mohrmann and colleagues found that null mutations in *polybromo* do not result in lethality (Mohrmann et al., 2004), and therefore, this result was expected. With the exception of *polybromo[32840]*, the RNAi lines that did not induce lethality were excluded from the study.

**Table 3. Percent survival of *Actin5C-GAL4* mediated knockdown of SWI/SNF subunits.**

| Gene | Stock # | Total Survival (% ± SE) | $n_{total}$ | Male Survival (% ± SE) | $n_{male}$ | Female Survival (% ± SE) | $n_{female}$ | $\chi^2$ | P |
|---|---|---|---|---|---|---|---|---|---|
| *mCherry* | 35785 | 80.2 ± 8.40 | 245 | 73.1 ± 18.4 | 116 | 87.0 ± 6.50 | 129 | 3.42 | 0.331 |
| *Act5C* | 42651 | 31.4 ± 36.2 | 46 | 31.2 ± 30.9 | 21 | 31.6 ± 41.5 | 25 | 12.5 | $5.8 \times 10^{-3}$ |
| | 101438 | 3.74 ± 1.75 | 46 | 4.17 ± 1.88 | 21 | 3.39 ± 1.70 | 25 | 191 | $<1.0 \times 10^{-4}$ |
| *Bap170* | 26308 | 1.70 ± 3.70 | 120 | 1.56 ± 4.76 | 65 | 1.85 ± 3.03 | 55 | 112 | $<1.0 \times 10^{-4}$ |
| | 34582 | 0.719 ± 1.15 | 140 | 0 | 61 | 1.28 ± 1.96 | 79 | 136 | $<1.0 \times 10^{-4}$ |
| *Bap55* | 24703 | 5.00 ± 4.40 | 147 | 1.61 ±1.85 | 63 | 7.69 ± 7.80 | 84 | 121 | $<1.0 \times 10^{-4}$ |
| | 31708 | 83.3 ± 23.3 | 77 | 85.2 ± 27.0 | 50 | 80.0 ± 29.3 | 27 | 0.653 | 0.884 |
| *Bap60* | 32503 | 0 | 122 | 0 | 65 | 0 | 57 | 122 | $<1.0 \times 10^{-4}$ |
| | 33954 | 17.8 ± 12.4 | 185 | 23.1 ± 15.8 | 96 | 12.7 ± 8.04 | 89 | 91.0 | $<1.0 \times 10^{-4}$ |
| *BCL7-like* | 35714 | 96.9 ± 13.2 | 128 | 90.3 ± 26.1 | 59 | 103 ± 34.5 | 69 | 0.167 | 0.983 |
| | 20410 | 43.6 ± 5.78 | 168 | 37.7 ± 14.7 | 73 | 48.4 ± 5.01 | 95 | 26.4 | $<1.0 \times 10^{-4}$ |
| *brm* | 37720 | 0.962 ± 0.790 | 105 | 2.04 ± 1.96 | 50 | 0 | 55 | 101 | $<1.0 \times 10^{-4}$ |
| | 34520 | 77.8 ± 15.6 | 208 | 61.7 ± 23.0 | 97 | 94.7 ± 21.3 | 111 | 5.54 | 0.137 |
| | 31712 | 0 | 61 | 0 | 27 | 0 | 34 | 42.0 | $<1.0 \times 10^{-4}$ |
| *CG10555* | 50606 | 98.0 ± 37.4 | 196 | 100 ± 66.3 | 88 | 96.4 ± 23.4 | 108 | 0.037 | 0.998 |
| | 105802 | 0 | 96 | 0 | 42 | 0 | 54 | 96.0 | $<1.0 \times 10^{-4}$ |
| *CG7154* | 37670 | 1.23 ± 1.15 | 82 | 2.63 ± 2.56 | 39 | 0 | 43 | 78.1 | $<1.0 \times 10^{-4}$ |
| | 107992 | 0.909 ± 0.850 | 111 | 1.82 ± 1.67 | 56 | 0 | 55 | 107 | $<1.0 \times 10^{-4}$ |
| *CG9650* | 23170 | 0 | 49 | 0 | 24 | 0 | 25 | 22.0 | $<1.0 \times 10^{-4}$ |
| | 40852 | 0 | 112 | 0 | 43 | 0 | 69 | 112 | $<1.0 \times 10^{-4}$ |
| | 104402 | 4.80 ± 3.30 | 175 | 10.9 ± 8.60 | 71 | 1.00 ± 0.900 | 104 | 146 | $<1.0 \times 10^{-4}$ |
| *Bap111* | 26218 | 1.41 ± 1.96 | 72 | 0 | 41 | 3.33 ± 6.67 | 31 | 68.1 | $<1.0 \times 10^{-4}$ |
| | 35242 | 3.55 ± 0.970 | 146 | 0 | 71 | 7.14 ± 2.61 | 75 | 127 | $<1.0 \times 10^{-4}$ |
| *e(y)3* | 32346 | 0 | 30 | 0 | 13 | 0 | 17 | 30.0 | $<1.0 \times 10^{-4}$ |
| | 105946 | 0 | 120 | 0 | 46 | 0 | 74 | 120 | $<1.0 \times 10^{-4}$ |
| *mor* | 110712 | 1.20 ± 1.33 | 168 | 2.63 ± 4.17 | 78 | 0 | 90 | 160 | $<1.0 \times 10^{-4}$ |
| | 6969 | 0.826 ± 0.930 | 122 | 0 | 58 | 1.59 ± 1.75 | 64 | 118 | $<1.0 \times 10^{-4}$ |
| *osa* | 38285 | 2.47 ± 1.55 | 83 | 2.78 ± 3.03 | 37 | 2.22 ± 1.75 | 46 | 75.2 | $<1.0 \times 10^{-4}$ |
| | 7810 | 2.13 ± 0.980 | 144 | 1.49 ± 2.08 | 68 | 2.70 ± 1.80 | 76 | 132 | $<1.0 \times 10^{-4}$ |
| *polybromo* | 32840 | 102 ± 12.2 | 198 | 81.5 ± 16.5 | 98 | 127 ± 7.79 | 100 | 2.46 | 0.482 |
| *Snr1* | 32372 | 4.04 ± 3.92 | 103 | 7.84 ± 9.52 | 55 | 0 | 48 | 88.2 | $<1.0 \times 10^{-4}$ |
| | 12644 | 53.8 ± 18.8 | 120 | 45.2 ± 12.8 | 45 | 59.6 ± 22.3 | 75 | 11.2 | 0.010 |

## 3.2 MB-specific knockdown of the SWI/SNF subunits results in aberrant mushroom body morphology

To investigate the role of the SWI/SNF complex in axon development, each of the 15 SWI/SNF subunits were knocked down in the MB using a collection of transgenic *UAS-RNAi* lines. Confocal stacks were examined to look for gross morphological phenotypes in the development of the *Drosophila* MB. To account for genetic background effects, knockdowns were compared to their corresponding genetic background control line (Appendix B). This analysis revealed four distinct phenotypic classes, including the appearance of missing α and β lobes, β-lobe fibers crossing the midline, extra dorsal projections and stunted γ-lobes (Appendix C).

Missing α and β lobes were observed at a low penetrance in both knockdowns and controls (Figure 7), whereas the β-lobe crossing phenotype was observed in nearly all genotypes (Figure 8). The appearance of missing α and β lobes appeared to be random, while the β-lobe crossing phenotype was highly penetrant in certain genotypes (*UAS-Bap60$^{33954}$*; P= 0.0140, *UAS-osa$^{38285}$*; P= 0.0494, *UAS-Bap170$^{34582}$*; P= 0.0297). In total, these phenotypes were observed in 81% of the knockdowns and 70% of the controls. The missing lobe and β-lobe crossing phenotypes were previously reported in a study looking at the genetic basis of natural variation in MB size, and it was suggested that they may be due to the random fixation of deleterious mutations affecting MB structure (Zwarts et al., 2015). Taken together, these findings suggest that the latter phenotypes are not the result of reduced SWI/SNF function.

MB-specific knockdown of *Bap60*, *Act5C, Snr1*, *CG9650*, *CG7154* and *e(y)3* also resulted in the appearance of extra dorsal projections adjacent to the MB α-lobe (Figure 9). A mild form of the extra dorsal projection phenotype was observed in controls at a low frequency. However, knockdown of several SWI/SNF genes caused a very severe and highly penetrant extra dorsal projection phenotype that was consistent between two RNAi lines for the same gene. This suggests that the moderate and severe forms of the extra dorsal projection phenotype are likely the result of SWI/SNF knockdown. Knockdown of *Bap60* resulted in a very strong and highly penetrant form of the extra dorsal projection phenotype using two different RNAi lines (*UAS-Bap60$^{32503}$*; P= 0.0021,

*UAS-Bap60$^{33954}$*; P= 0.0007). Knockdown of *Act5C* using two independent RNAi constructs also resulted in the appearance of extra dorsal projections adjacent to the α lobe. However, a significant phenotype was only observed for one of the two RNAi lines tested, with the other approaching significance (*UAS-Act5C$^{101438}$*; P= 0.0007; *UAS-Act5C$^{42651}$*; P= 0.0560). A significant increase in the frequency of the extra dorsal projection phenotype was also observed for one of two RNAi lines targeting *Snr1* (*UAS-Snr1$^{32372}$*; P= 0.0196). Besides the core subunits, a significant increase in the frequency of the extra dorsal projection phenotype was observed following knockdown of three additional genes. A strong phenotype was observed following knockdown of *CG9650* and *CG7154* using a single RNAi construct (*UAS-CG9650$^{40852}$*; P= 0.0002, *UAS-CG7154$^{107992}$* ; P= 0.0007), while knockdown of the *PBAP*-specific gene *e(y)3* resulted in the appearance of a very severe and highly penetrant form of the extra dorsal projection phenotype (*UAS-e(y)3$^{32346}$*; P= 0.0042, *UAS-e(y)3$^{105946}$*; P= 0.0007) that was consistent using two independent RNAi stocks. Conversely, no phenotype was observed following knockdown of the *BAP*-specific gene, *osa*. Knockdown of *Act5C*, *Bap60* and *Snr1* using a single RNAi construct also resulted in the formation of stunted γ-lobes in nearly all brains examined (Figure 10). In comparison to the appropriate genetic background controls, a significant increase in the frequency of the stunted γ-lobe phenotype was observed following knockdown of *Act5C* using two independent RNAi constructs (*UAS-Act5C$^{42651}$*, *UAS-Act5C$^{101438}$*; P= 0.0007). A significant increase in the frequency of the stunted γ-lobe phenotype was also observed for knockdown of *UAS-Bap60$^{33954}$* (P= 0.0007) and *UAS-Snr1$^{32372}$* (P= 0.0007), whereas no significant phenotype was observed for *UAS-Bap60$^{32503}$* or *UAS-Snr1$^{12644}$*. The discrepancy between the two *Snr1* RNAi lines could be explained by the results of the lethality assay. We observed a 53% survival rate for *UAS-Snr1$^{12644}$*, compared to 4% for *UAS-Snr1$^{32372}$* (Table 3), suggesting that *UAS-Snr1$^{12644}$* may induce a weaker gene knockdown. Overall, these findings suggest that the SWI/SNF complex is required for axon morphogenesis in the *Drosophila* MB. Furthermore, the presence of a strong and consistent phenotype between two RNAi lines for knockdown of *e(y)3* suggests that the PBAP form of the *Drosophila* SWI/SNF complex may play a key role in the molecular mechanisms underlying the observed phenotypes.
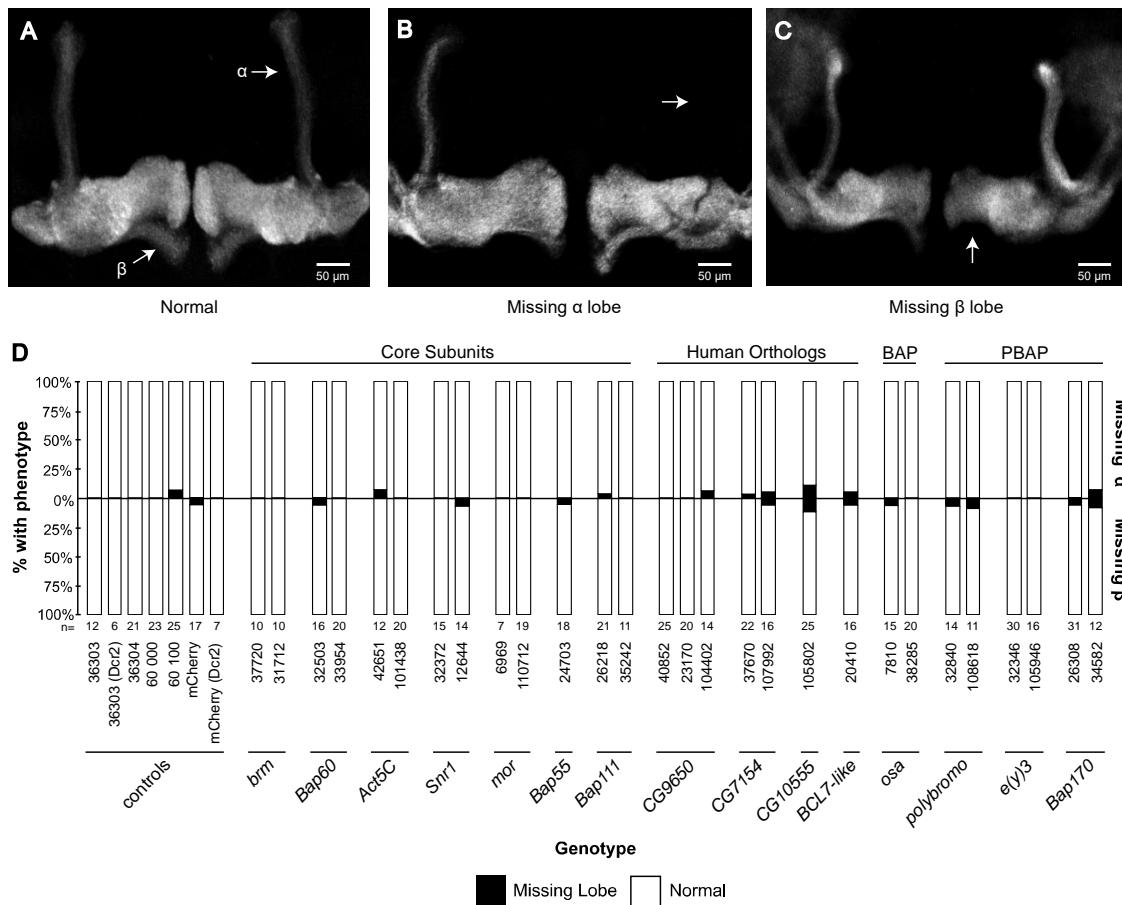
**Figure 7. Missing α and β lobes were observed at a low penetrance in both knockdowns and controls.**

Confocal projections show **(A)** normal MB morphology, **(B)** the missing α-lobe phenotype and **(C)** the missing β-lobe phenotype. **(D)** Bar plots indicate the total percentage of brains exhibiting the missing α-lobe phenotype (above x-axis) and missing β-lobe phenotype (below x-axis). The total number of flies analyzed for each genotype is indicated below the bar graph in the row labelled "n".
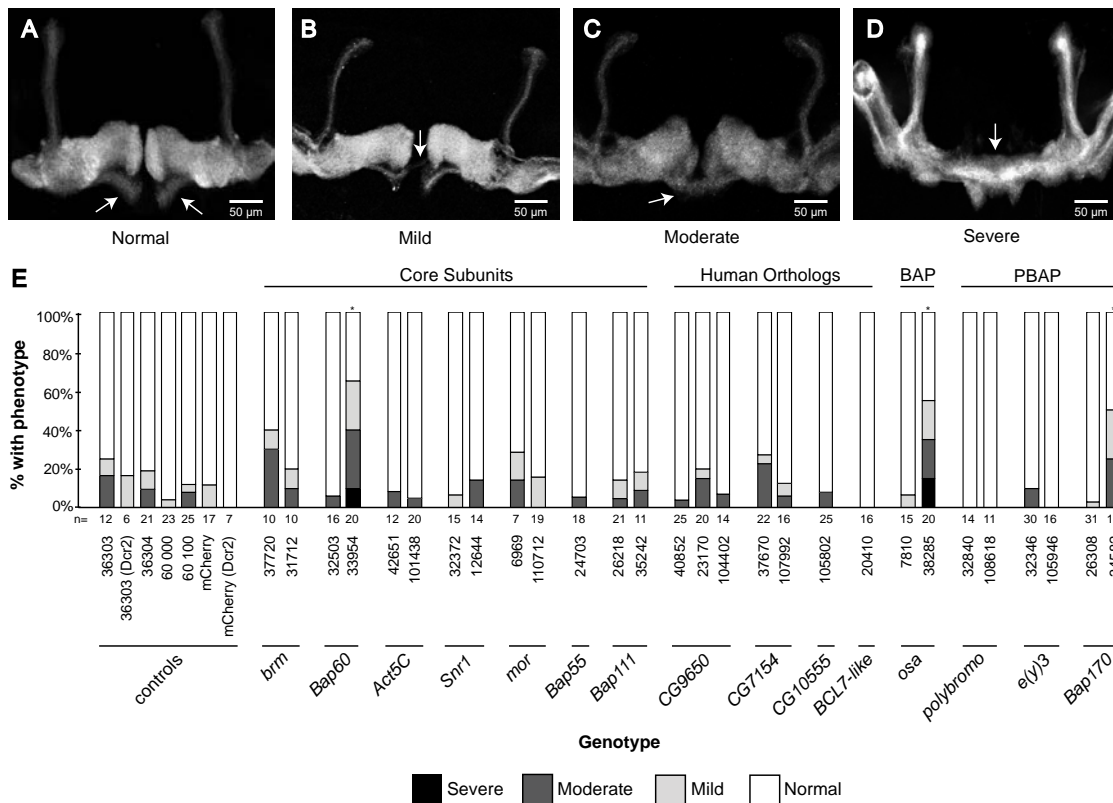
**Figure 8. The appearance of β-lobe fibers crossing the midline was observed at a variable penetrance in both knockdowns and controls.**

The β-lobe crossing phenotype was qualitatively classified into four categories to account for the observed variation in phenotype severity. Confocal projections show **(A)** normal MB morphology, in addition to the **(B)** mild, **(C)** moderate and **(D)** severe forms of the β-lobe crossing phenotype. **(E)** Bar plot shows the total percentage of brains exhibiting normal MB morphology (white), in addition to the mild (light gray), moderate (dark gray) and severe (black) forms of the β-lobe crossing phenotype. The total number of flies analyzed for each genotype is indicated below the bar graph in the row labelled "n". The Fisher's exact test (two-tailed) was used to compare the proportion of MBs exhibiting abnormal morphology (sum of mild, moderate and severe proportions) to the proportion exhibiting normal morphology between each knockdown and the appropriate control (Bonferroni-Dunn test for multiple comparisons). Asterisks indicate significance (* P≤0.05).
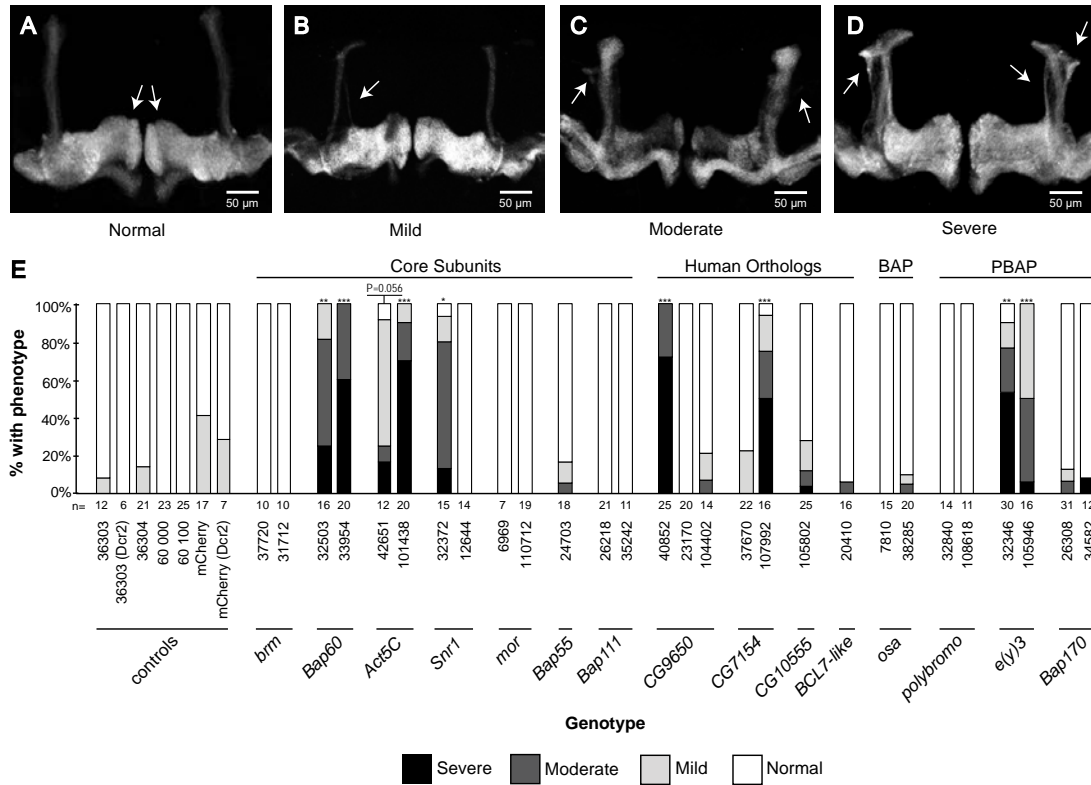
**Figure 9. MB-specific knockdown of the SWI/SNF subunits resulted in the formation of extra dorsal projections adjacent to the α-lobe.**

The extra dorsal projection phenotype was qualitatively classified into four categories to account for the observed variation in phenotype severity. Confocal projections show **(A)** normal MB morphology, in addition to the **(B)** mild, **(C)** moderate and **(D)** severe forms of the extra dorsal projection phenotype. **(E)** Bar plot shows the total percentage of brains exhibiting normal MB morphology (white), in addition to the mild (light gray), moderate (dark gray) and severe (black) forms of the extra dorsal projection phenotype. The total number of flies analyzed for each genotype is indicated below the bar graph in the row labelled "n". The Fisher's exact test (two-tailed) was used to compare the proportion of MBs exhibiting abnormal morphology (sum of mild, moderate and severe proportions) to the proportion exhibiting normal morphology between each knockdown and the appropriate control (Bonferroni-Dunn test for multiple comparisons). Asterisks indicate significance (* P≤0.05, ** P≤0.01, *** P≤0.001).
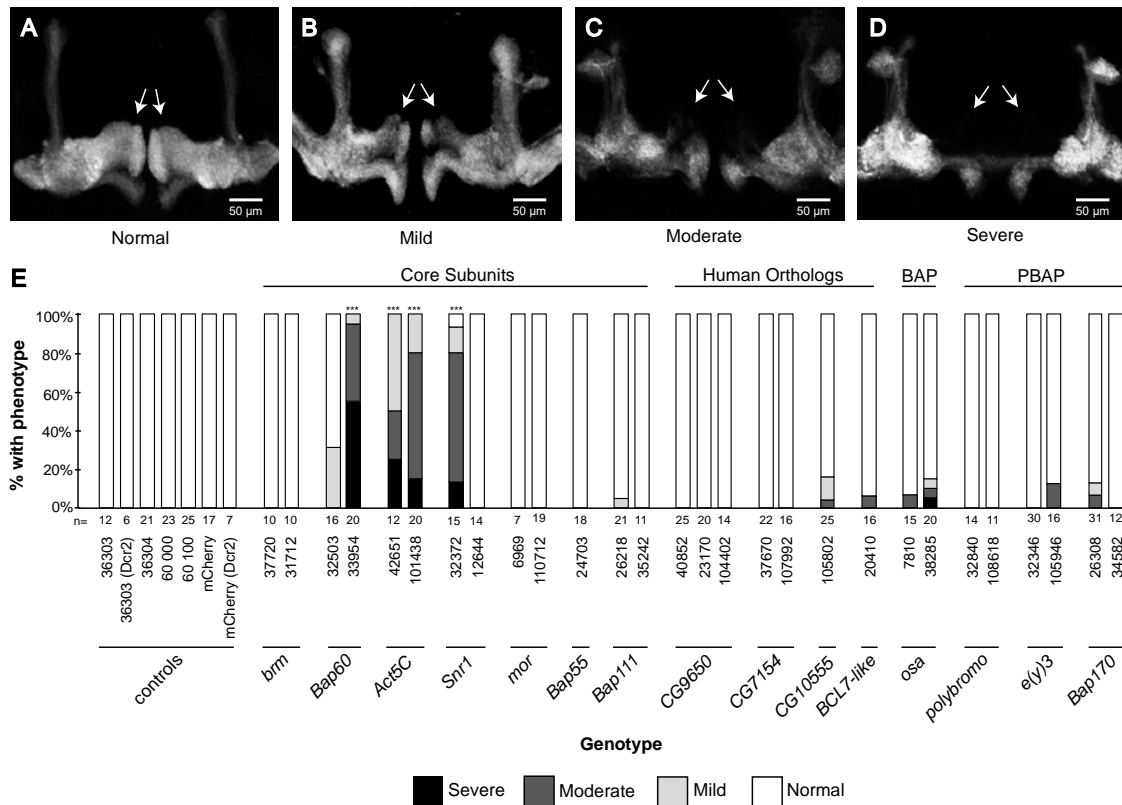
**Figure 10. MB-specific knockdown of the SWI/SNF subunits resulted in the appearance of stunted γ-lobes.**

The stunted γ-lobe phenotype was qualitatively classified into four categories to account for the observed variation in phenotype severity. Confocal projections show **(A)** normal MB morphology, in addition to the **(B)** mild, **(C)** moderate and **(D)** severe forms of the stunted γ-lobe phenotype. **(E)** Bar plot shows the total percentage of brains exhibiting normal MB morphology (white), in addition to the mild (light gray), moderate (dark gray) and severe (black) forms of the stunted γ-lobe phenotype. The total number of flies analyzed for each genotype is indicated below the bar graph in the row labelled "n". The Fisher's exact test (two-tailed) was used to compare the proportion of MBs exhibiting abnormal morphology (sum of mild, moderate and severe proportions) to the proportion exhibiting normal morphology between each knockdown and the appropriate control (Bonferroni-Dunn test for multiple comparisons). Asterisks indicate significance (*** $P \leq 0.001$).

### 3.2.1    The appearance of extra dorsal projections likely results from defects in γ-neuron remodelling

Knockdown of several SWI/SNF subunits resulted in the appearance of extra dorsal projections adjacent to the MB α-lobe. Several studies have reported the appearance of a similar phenotype arising from defects in γ pruning, raising the possibility that the extra dorsal projection phenotype observed in this study may be the result of defective γ-neuron remodelling (Boulanger et al., 2011; Lai et al., 2016). To investigate this possibility, knockdown was induced using *MB607B-GAL4*. Expression studies have revealed that the *MB607B* driver expresses GAL4 in approximately 75 cells located within the main MB calyx and the dorsal portion of the MB γ-lobe (Aso et al., 2014). *MB607B-GAL4* induced knockdown of *Bap60*, *Snr1* and *e(y)3* resulted in the appearance of MB γ neurons projecting their axons into the dorsal direction of the adult brain (Figure 11). This finding indicates that the extra dorsal projection phenotype is due to improper development of the MB γ neurons, ruling out a possible defect in axon guidance of the MB α/β neurons. Overall, these results demonstrate that knockdown of *Bap60*, *Snr1* and the *PBAP*-specific gene *e(y)3* caused defects in either the axon pruning of the larval specific MB γ neurons or the inappropriate re-extension of the adult specific MB γ neurons.
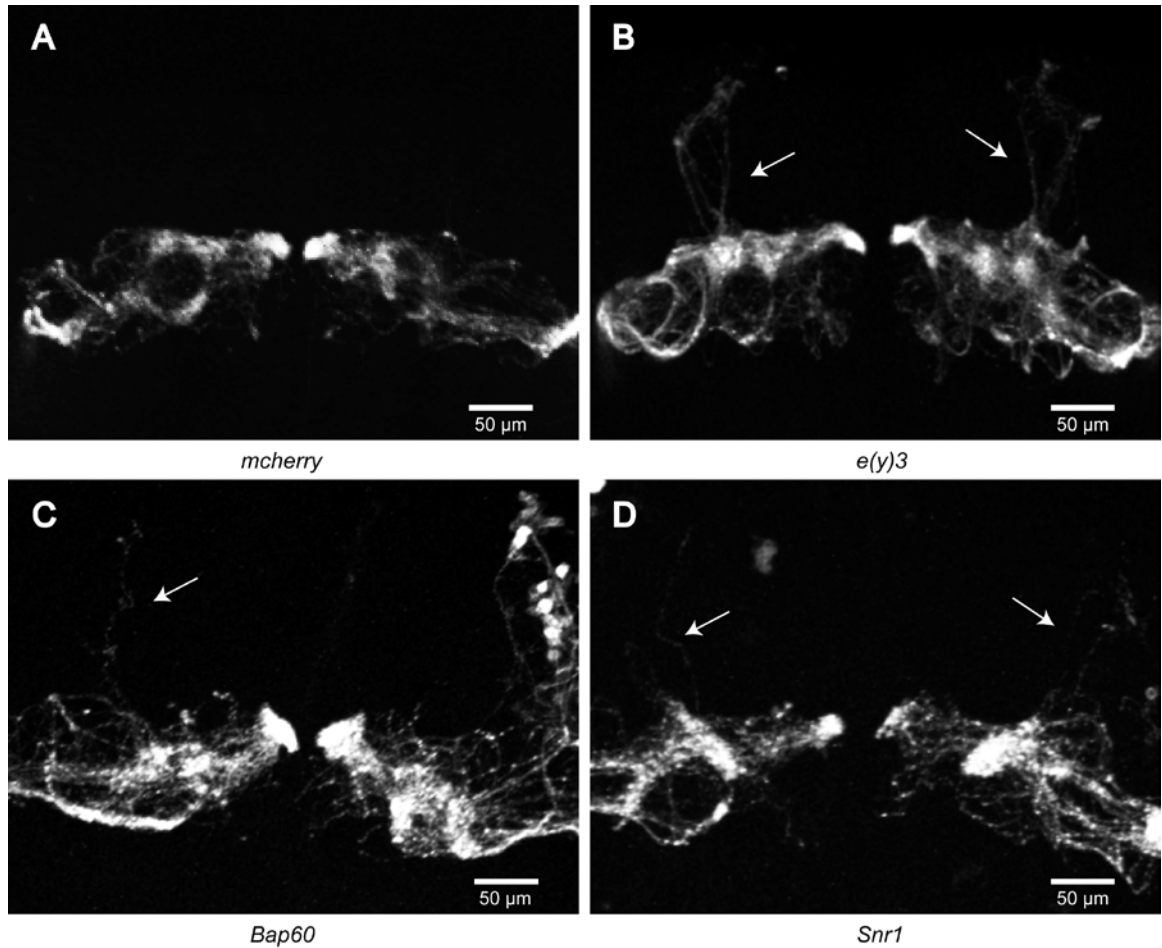
**Figure 11. Knockdown of *e(y)3*, *Bap60* and *Snr1* using *MB607B-GAL4* revealed defects in γ-neuron remodelling.**

The *MB607B-GAL4* driver was used to induce RNAi knockdown in the MB γ neurons. *MB607B-GAL4* was also used to drive the expression of UAS-mCD8::GFP for visualization of the adult specific MB γ neurons. Confocal projections show the axonal projection patterns of the MB γ neurons in **A)** control, **B)** *UAS-e(y)3[32346]*, **C)** *UAS-Bap60[32503]* and **D)** *UAS-Snr1[32372]* genotypes. **A)** Dorsally projecting γ neurons were not observed in the mCherry RNAi hairpin control. **(B-D)** Knockdown of *UAS-e(y)3[32346]*, *UAS-Bap60[32503]* and *UAS-Snr1[32372]* resulted in the appearance of dorsally projecting γ neurons.

## 3.3 MB-specific knockdown of the SWI/SNF components resulted in the appearance of faint γ-lobes

*R14H06-GAL4* is specifically expressed in the α, β and γ neurons of the *Drosophila* MB (Jenett et al., 2012). In controls, GFP expression is strongest within the γ-lobe and weakest within the α/β lobes (Refer to Figure 12A). Several SWI/SNF knockdown genotypes showed the appearance of faint γ-lobes that were otherwise morphologically normal (Refer to Figure 12B). This observation suggests that knockdown of certain SWI/SNF components may result in either loss of the MB γ neurons, or an increase in the number of α/β neurons. In order to quantitatively assess the relative γ-lobe intensity across genotypes, pixel intensity sampling was performed at various different locations within the γ and α-lobes of the MB (Refer to Figure 6). The ratio of the signal intensity of the MB γ-lobe to that of the α-lobe was calculated for each genotype and compared to the mCherry control.

On average, the fluorescent signal within the γ-lobe of the controls is more than 2 fold greater than that of the α-lobe (Refer to Figure 12C, control). Due to the severe stunted γ-lobe phenotype observed following knockdown of A*ct5C*, the γ-lobes could not be quantified. Furthermore, signal intensity could not be quantified for knockdown of *Bap60$^{33954}$* due to the severely stunted γ-lobe phenotype mentioned above. However, images were quantified for all other RNAi knockdown genotypes. For the core SWI/SNF components, a significant decrease in the relative signal intensity of the γ-lobe was observed following knockdown of *brm* (*UAS-brm$^{37720}$*; P= 0.0052, *UAS-brm$^{31712}$*; P= 0.0001) and *Bap111* (*UAS-Bap111$^{26218}$*, *UAS-Bap111$^{35242}$*; P= 0.0001) using two independent RNAi lines. Knockdown of *UAS-Bap60$^{32503}$* (P= 0.0001), *UAS-Snr1$^{32372}$* (P= 0.0041) and *UAS-mor$^{110712}$* (P= 0.0001) using a single RNAi construct also resulted in a significant reduction in relative γ-lobe intensity. No significant difference was observed following knockdown of *Bap55*, but this could only be tested using a single RNAi line. A significant reduction in relative γ-lobe intensity was also observed upon knockdown of the human ortholog *CG9650* using two out of three RNAi lines tested. However, no phenotype was observed for any of the other human orthologs. Notably, a very strong and consistent phenotype was observed following knockdown of the *BAP*-specific gene *osa* using two independent RNAi lines (*UAS-osa$^{7810}$*, *UAS-osa$^{38285}$*; P=

0.0001).   Conversely, knockdown of the *PBAP*-specific genes caused a significant reduction in relative signal intensity for *UAS-Bap170*[26308] (P= 0.0001), *UAS-polybromo*[32840] (P= 0.0001) and *UAS-e(y)*[32346] (P= 0.0235) using one of two RNAi lines tested.  Due to the fact that knockdown of the *BAP*-specific gene resulted in the strongest and most consistent phenotype,  data suggests that the γ fade phenotype may be due to loss of the BAP complex.
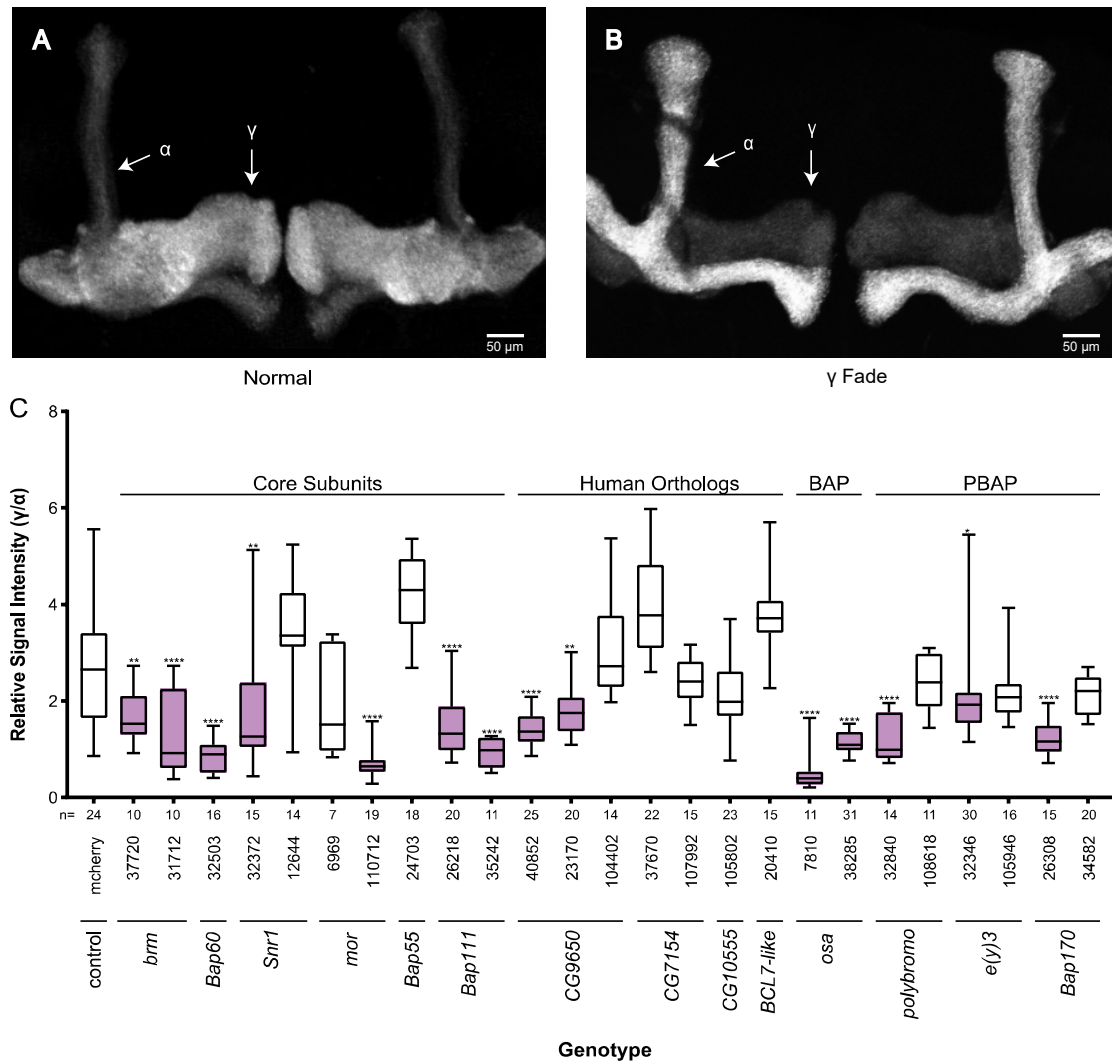
**Figure 12. MB-specific knockdown of the SWI/SNF subunits caused a reduction in relative γ-lobe intensity.**

*R14H06-GAL4* is expressed in the adult α, β and γ neurons of the *Drosophila* MB. **(A)** *R14H06*-driven GFP expression is strongest in the γ-lobe of controls. **(B)** Confocal projection showing an example of the γ fade phenotype. **(C)** Box plot displays the distribution of relative signal intensity values for SWI/SNF knockdowns and the mCherry RNAi hairpin control. The total number of flies analyzed for each genotype is indicated below the bar graph in the row labelled "n". Differences between knockdowns and the mCherry control were conducted using one way ANOVA with the Dunnet test for selected multiple comparisons (n=25). Asterisks indicate significance (* P≤0.05, ** P≤0.01, *** P≤0.001, **** P≤0.0001).

# Chapter 4

# 4    DISCUSSION

In this study, I have analyzed the role of the SWI/SNF chromatin remodelling complex in the axon development of the *Drosophila* MB.  The results of this study have revealed two distinct phenotypes resulting from loss of SWI/SNF function.  In particular, defects in γ-neuron remodelling were observed following MB-specific knockdown of *Bap60*, *Snr1* and *e(y)3*, while a reduction in the relative signal intensity of the γ-lobe was observed following knockdown of several other SWI/SNF components.  Knockdown of the *PBAP*-specific gene, *e(y)3,* caused the strongest and most consistent defect in γ-neuron remodelling amongst all of the genes analyzed in this study.  In contrast, knockdown of the *BAP*-specific gene, *osa*, resulted in the strongest reduction in relative signal intensity among the 15 SWI/SNF genes.  These findings suggest that the PBAP form of the *Drosophila* SWI/SNF complex may be required for γ-neuron remodelling, whereas the BAP form of the complex may play a more important role in the mechanisms underlying the observed reduction in γ-lobe intensity.

## 4.1   The *Drosophila* SWI/SNF complex is required for the remodelling of the MB γ neurons

During metamorphosis in *Drosophila*, the MB γ neurons undergo extensive remodelling as the nervous system transitions from its larval to adult form.  Prior to puparium formation, the γ neurons direct their axons into both the dorsal and medial directions (Lee et al., 1999).  Approximately 6 hours after the onset of puparium formation, axon fragmentation begins to reduce the axonal projections of the MB γ neurons back to the peduncle (Hakim et al., 2014).  Following the completion of axon pruning at approximately 18 hours APF, the γ neurons initiate re-extension of their axons into the medial lobe at 24 hours APF (Hakim et al., 2014).

In this project, I have demonstrated that the appearance of extra dorsal projections following knockdown of *e(y)3*, *Bap60* and *Snr1* is likely the result of defects in γ remodelling (Figure 11).  However, the exact cause of the remodelling defect is unclear.  Several studies have shown that defects in axon pruning during *Drosophila*

metamorphosis result in the appearance of extra dorsal projections adjacent to the α-lobe (Boulanger et al., 2011; Lai et al., 2016). It is also possible that the remodelling defects observed in this study may have resulted from inappropriate axon re-extension of the adult specific MB γ neurons. In order to differentiate between these two possibilities, future studies using the *MB607B-GAL4* driver should assess MB morphology at the larval, pupal and adult stages of development. An axon pruning defect could then be confirmed by examining MB morphology at 18 and 24 hours APF, when pruning is complete. Conversely, the absence of pruning defects at this time point would indicate that the remodelling defect observed in this study was the result of improper axon re-extension. Future studies should investigate these possibilities in order to gain a further understanding of the mechanisms underlying the observed defects in neuronal remodelling.

## 4.2 Regulation of γ-neuron remodelling by the PBAP form of the SWI/SNF complex

The *Drosophila* SWI/SNF complex is known to exist in two different forms, each characterized by the presence of a specific set of accessory subunits. The BAP complex is defined by the presence of the BAP-specific subunit Osa, whereas the PBAP complex is characterized by the presence of the PBAP-specific subunits, Polybromo, Bap170 and E(y)3 (Mohrmann et al., 2004). In this study, MB-specific knockdown of *e(y)3* resulted in the appearance of severe defects in γ-neuron remodelling. Conversely, the BAP-specific subunit, Osa, appeared to be unaffected. These findings suggest that the PBAP form of the *Drosophila* SWI/SNF complex may play a more important role in the transcriptional regulation required for remodelling of the MB γ neurons.

Several previous studies have shown that γ-neuron remodelling is dependent on ecdysone signalling (Lee et al., 2000; Schubiger et al., 1998). The EcR-B1 isoform is specifically expressed in the γ neurons of the larval MB, and its expression has been shown to be required for the remodelling of the γ neurons during metamorphosis (Lee et al., 2000). Several lines of evidence suggest that the defects in γ-neuron remodelling observed in this study may be caused by defects in ecdysone signalling. First, transcriptome analysis revealed that mutations in *Snr1* result in overexpression of the late

expressed ecdysone inducible genes (Zraly et al., 2006). Second, the *e(y)3* encoded protein, formerly known as SAYP, was shown to interact with the DHR3 nuclear receptor to activate gene transcription during the embryonic and pupal stages of development (Vorobyeva et al., 2011). The expression of the DHR3 receptor is directly activated by a pulse of ecdysone at the onset of metamorphosis (Lam et al., 1997), and its activation has been suggested to play a key role in the regulation of several ecdysone response genes (Carney et al., 1997). Following the ecdysone-induced activation of DHR3, ChIP experiments revealed that DHR3 and SAYP cooperatively bind to the promoters of several SAYP-dependent genes to activate their expression (Vorobyeva et al., 2011). One well characterized DHR3 target gene is the Ftz-f1 transcription factor which is required for the induction of EcR-B1 expression at the onset of metamorphosis (Lam et al., 1997). A study investigating the role of SAYP in *ftz-f1* transcription found that SAYP is required for the temporal regulation of *ftz-f1* activation throughout metamorphosis (Vorobyeva et al., 2012). Accordingly, loss of *ftz-f1* has been shown to cause remodelling defects in the *Drosophila* MB (Boulanger et al., 2011; Lam et al., 1997). Taken together, it is possible that the PBAP-specific subunit, E(y)3, may be required for γ-neuron remodelling through the regulation of *ftz-f1* transcription in cooperation with DHR3 (Figure 13). The DHR3 receptor is known to play a key role in *Drosophila* metamorphosis, yet its role in neuronal remodelling has yet to be determined. It would be interesting to see if RNAi-mediated knockdown of the DHR3 receptor causes defects in neuronal remodelling, similar to that of *e(y)3, ftz-f1* and *EcR-B1* (Boulanger et al., 2011; Lee et al., 2000). Overall, these findings suggest that the PBAP complex may interact with the ecdysone signalling pathway to induce γ neuronal remodelling.
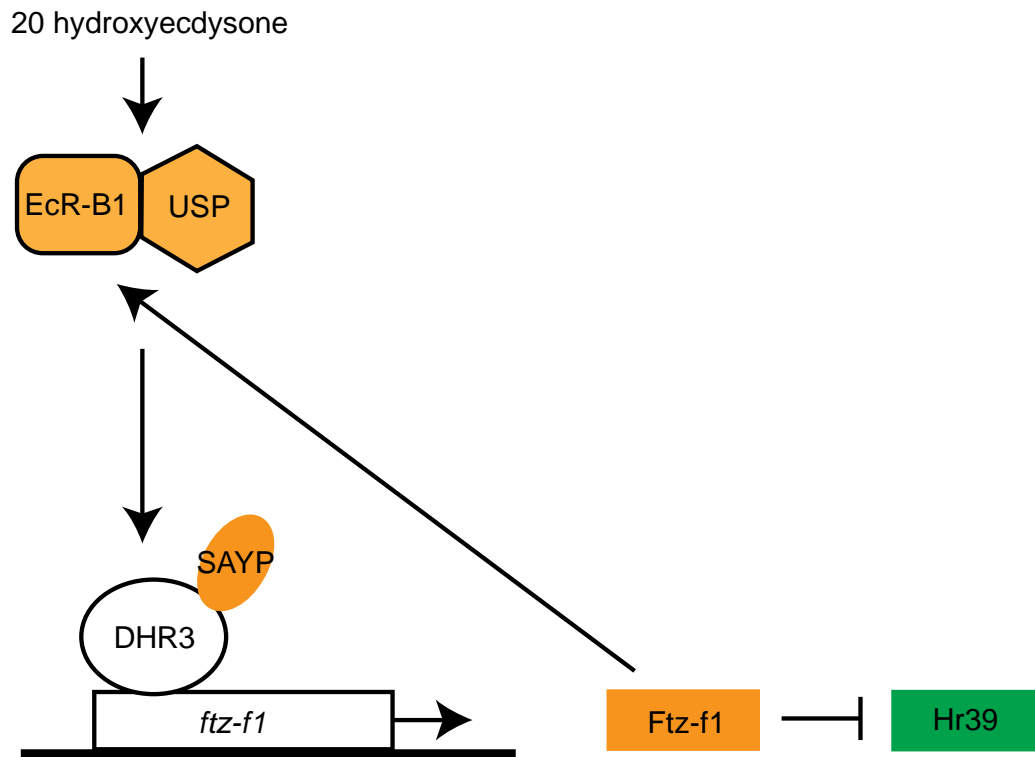
**Figure 13. Model of *ftz-f1* gene activation mediated by the interaction between DHR3 and SAYP.**

During metamorphasis, the insect molting hormone, 20-hydroxyecdysone, binds to the EcR-B1/USP receptor to initiate ecdysone signalling. Upon ecdysone induced activation, DHR3 binds to the promoter of the *ftz-f1* gene and recruits the SAYP transcriptional co-activator. The interaction of SAYP and DHR3 initiates the transcriptional activation of *ftz-f1*, resulting in production of the Ftz-f1 protein. Activation of Ftz-F1 leads to the repression of the Hr39 nuclear receptor and upregulation of the EcR-B1 isoform. Highlighted proteins have been shown to be implicated in γ-neuron remodelling as a result of loss of function (orange) or gain of function (green) mutations (Boulanger et al., 2011; Lee et al., 2000).

## 4.3 Regulation of mushroom body development by the BAP form of the SWI/SNF complex

The *R14H06* driver is most strongly expressed in the γ-lobe, represented by an approximate threefold increase in GFP signal intensity compared that that of the α-lobe (Refer to Figure 12C, control). MB-specific knockdown of several SWI/SNF components caused a relative decrease in signal intensity of the γ-lobe in comparison to the α-lobe, such that the α-lobe appears brighter than the γ-lobe. It is possible that the reduction in relative signal intensity may have resulted from loss of the MB γ neurons, or alternatively, an increase in the number of α/β neurons.

SWI/SNF knockdown may have resulted in decreased cell viability of the MB γ neurons and the initiation of cell death, ultimately leading to loss of the MB γ neurons. A previous study in *Drosophila* found that null mutations in *brm* result in decreased cell viability and cause defects in peripheral nervous system development (Elfring et al., 1998). In line with these findings, I observed a significant reduction in relative signal intensity of the γ-lobe following knockdown of *brm* using two independent RNAi lines. Future studies should investigate this possibility by immunostaining for the active form of caspase-9, an active marker of apoptosis (McIlwain et al., 2013). In addition, it is also possible that the observed decrease in relative signal intensity may have resulted from defects in axon guidance or re-extension. I have demonstrated that knockdown of several SWI/SNF components resulted in defects in axon morphogenesis and γ-neuron remodelling. The remodelling of the MB γ neurons involves degeneration of the larval specific axons, followed by re-extension of the adult specific axonal projections. Loss of SWI/SNF function in the MB may have caused defects in axon re-extension, such that a proportion of the MB γ neurons failed to re-extend their axons past the peduncle. As a result, a reduced number of γ neurons would be present in the MB γ lobe of the adult. Notably, the results of my study found that knockdown of several SWI/SNF components resulted in the appearance of small and stunted γ-lobes. Due to the severity of the stunted γ-lobe phenotype observed following knockdown of *Act5C*[42651], *Act5C*[101438] and *Snr1*[33954], I was unable to quantitatively measure the relative signal intensity of the γ-lobe for these genotypes. However, knockdown of several other genes resulted in both the appearance of stunted γ-lobes and a decrease in the relative signal intensity of the γ-lobe.

These findings suggest that the stunted γ-lobe phenotype observed in this study may represent a more severe phenotype arising from loss of the MB γ neurons.

An alternative explanation for the reduction in relative signal intensity of the γ-lobe is that SWI/SNF knockdown caused an increase in the number of α/β neurons. MB development involves the sequential generation of three different types of neurons, each of which arise from the division of a single neuroblast cell (Lee et al., 1999). It is possible that the sequential generation of the MB neurons may be maintained by changes in gene expression mediated by the SWI/SNF complex. Therefore, it is possible that SWI/SNF knockdown may have resulted in dysregulation of the signaling pathways required for maintaining cell fate throughout MB morphogenesis. As a result, knockdown may have induced trans-differentiation in the post-mitotic neurons of the MB, such that the γ neurons undergo a change in cell fate to become α/β neurons.

In this study, MB-specific knockdown of *osa* caused a very strong and consistent decrease in the relative signal intensity of the MB γ-lobe. The results of a previous study demonstrated that the BAP-specific subunit Osa modulates the function of the BAP complex via interactions with Brm and Snr1 (Collins et al., 1999), both of which resulted in a significant reduction in relative signal intensity of the γ lobe following knockdown. The BAP form of the SWI/SNF complex has been shown to be involved in the regulation of cell cycle control. However, the role of this complex in post-mitotic neurons is less clear (Moshkin et al., 2007). It is possible that the BAP complex plays a widespread role in cellular viability and the maintenance of cellular identity. To better understand the role of the BAP complex in post-mitotic neural development, future studies should be performed that specifically target the BAP-specific subunit, Osa.

## 4.4   Research limitations

RNAi is an effective method for studying gene function in *Drosophila*. However, RNAi technology is limited by the potential for insufficient knockdown and off-target effects. As an estimate of knockdown efficiency, I used a lethality assay to measure percent survival following ubiquitous RNAi knockdown. The results of the lethality assay revealed five RNAi lines which showed no significant reduction in percent survival as compared to expected values. As a result, those RNAi lines were deemed ineffective

and eliminated from the study. However, the lethality assay does not provide any information regarding the overall expression level of the protein following knockdown. Therefore, it is possible that ubiquitous knockdown may have resulted in lethality due to false positives that arise from off target effects. To better quantify RNAi-mediated knockdown efficiency in these lines, future studies should validate the RNAi lines used in this study via qPCR and immunohistochemical analyses.

To control for potential off-target effects, I aimed to knockdown each SWI/SNF component using a minimum of two RNAi lines that target different regions of the endogenous mRNA. In doing so, consistent results between multiple RNAi lines would act as a key method of validation for any phenotypes observed following gene knockdown. However, I was only able to test one RNAi line for knockdown of *Bap55*, *BCL7-like* and *CG10555*. Therefore, it is difficult to make any strong conclusions about the results obtained from knockdown of these genes. Although the remaining SWI/SNF components were knocked down using multiple RNAi lines, some inconsistencies were observed between two RNAi lines for the same gene. However, overall, consistent results were observed between two RNAi lines targeting the same gene in 85% of the comparisons made in this thesis. Most of the inconsistencies came from the gamma fade analysis, which showed inconsistent results between RNAi lines at a rate of 50% (Section 3.3). In contrast, the analyses aimed at identifying gross defects in MB morphology resulted in an overall consistency rate of 92% (Section 3.2). As a result, the data obtained from the gamma fade analysis will require additional validation before strong conclusions can be made. Despite the limitations associated with RNAi, my results generally demonstrate a high rate of consistency in identifying developmental phenotypes in the *Drosophila* MB.

## 4.5 Conclusions, research implications and future directions

In this study, I have identified a number of phenotypes resulting from the loss of SWI/SNF function in the *Drosophila* MB. These results demonstrate that the SWI/SNF complex is required for axon morphogenesis in *Drosophila*, providing novel insight into the role of this epigenetic regulatory complex in the nervous system. Furthermore, the results of this study suggest that the BAP and PBAP forms of the *Drosophila* SWI/SNF

complex may play distinct roles in *Drosophila* neural development. However, the mechanisms through which the SWI/SNF complex regulates axon morphogenesis in the *Drosophila* MB have yet to be discovered. To better understand the molecular role of the SWI/SNF complex in neurodevelopment, future studies should aim to identify the neuron specific target genes affected by MB-specific knockdown of the SWI/SNF components.

The SWI/SNF complex is highly conserved between humans and *Drosophila* (Son & Crabtree, 2014). This suggests that the results attained in my study may provide evidence towards a potential role for the SWI/SNF complex in the human brain. Previous studies have identified a common role for the SWI/SNF complex in both *Drosophila* and mammalian neurons (Lessard et al., 2007; Wu et al., 2007). In this project, I have identified defects in neuronal remodelling following knockdown of *e(y)3*, *Bap60* and *Snr1* in the *Drosophila* MB. Notably, the mammalian ortholog of *e(y)3* has been shown to be required for the transition of neural progenitors to post-mitotic neurons (Lessard et al., 2007). In addition, mutations in the human orthologs of *Bap60* and S*nr1* have been implicated in ID (*SMARCB1*, *SMARCD1*) (Santen et al., 2013; Tsurusaki et al., 2012; Wieczorek et al., 2013). Future studies in *Drosophila* should aim to uncover the cellular and molecular mechanisms underlying SWI/SNF induced defects in axon development. Over the long term, this may enable hypothesis driven research using patient derived induced pluripotent stem cell models for ID. Ultimately, a greater understanding of the molecular mechanisms underlying ID will provide the first step towards the development of therapies.

# 5   REFERENCES

Adams, M.D., Celniker, S.E., Holt, R.A., Evans, C.A., Gocayne, J.D., Amanatides, P.G., Scherer, S.E., Li, P.W., Hoskins, R.A., Galle, R.F., et al. (2000). The Genome Sequence of *Drosophila melanogaster*. Science *287*, 2185–2195.

American Psychiatric Association. (2013). Diagnostic and Statistical Manual of Mental Disorders. Arlington, VA.

Amir, R.E., Van den Veyver, I.B., Wan, M., Tran, C.Q., Francke, U., and Zoghbi, H.Y. (1999). Rett syndrome is caused by mutations in X-linked *MECP2*, encoding methyl-CpG-binding protein 2. Nat. Genet. *23*, 185–188.

Araújo, S.J., and Tear, G. (2003). Axon guidance mechanisms and molecules: lessons from invertebrates. Nat. Rev. Neurosci. *4*, 910–922.

Aso, Y., Hattori, D., Yu, Y., Johnston, R.M., Iyer, N.A., Ngo, T.–T., Dionne, H., Abbott, L.F., Axel, R., Tanimoto, H., et al. (2014). The neuronal architecture of the mushroom body provides a logic for associative learning. eLife *3*, e04577.

Awasaki, T., and Lee, T. (2011). Orphan nuclear receptors control neuronal remodeling during fly metamorphosis. Nat. Neurosci. *14*, 6–7.

Bachmann, A., and Knust, E. (2008). The Use of P-Element Transposons to Generate Transgenic Flies. Methods Mol. Biol. *420*, 61–77.

Barski, A., Cuddapah, S., Cui, K., Roh, T.-Y., Schones, D.E., Wang, Z., Wei, G., Chepelev, I., and Zhao, K. (2007). High-Resolution Profiling of Histone Methylations in the Human Genome. Cell *129*, 823–837.

Berger, S.L., Kouzarides, T., Shiekhattar, R., and Shilatifard, A. (2009). An operational definition of epigenetics. Genes Dev. *23*, 781–783.

Bischof, J., Maeda, R.K., Hediger, M., Karch, F., and Basler, K. (2007). An optimized transgenesis system for *Drosophila* using germ-line-specific φC31 integrases. Proc. Natl. Acad. Sci. U.S.A *104*, 3312-3317.

Boulanger, A., Clouet-Redt, C., Farge, M., Flandre, A., Guignard, T., Fernando, C., Juge, F., and Dura, J.-M. (2011). *ftz-f1* and *Hr39* opposing roles on *EcR* expression during *Drosophila* mushroom body neuron remodeling. Nat. Neurosci. *14*, 37–44.

Brand, A.H., and Perrimon, N. (1993). Targeted gene expression as a means of altering cell fates and generating dominant phenotypes. Development *118*, 401–415.

Bultman, S., Gebuhr, T., Yee, D., La Mantia, C., Nicholson, J., Gilliam, A., Randazzo, F., Metzger, D., Chambon, P., Crabtree, G., et al. (2000). A *Brg1* Null Mutation in

the Mouse Reveals Functional Differences among Mammalian SWI/SNF Complexes. Mol. Cell *6*, 1287–1295.

Castle, W.E. (1906). Inbreeding, Cross-breeding and Sterility in Drosophila. Science *23*, 153.

Carney, G.E., Wade, A.A., Sapra, R., Goldstein, E.S., and Bender, M. (1997). *DHR3*, an ecdysone-inducible early-late gene encoding a *Drosophila* nuclear receptor, is required for embryogenesis. Proc. Natl. Acad. Sci. U.S.A *94*, 12024-12029.

Castro, J.P., and Carareto, C.M.A. (2004). *Drosophila melanogaster P* transposable elements: mechanisms of transposition and regulation. Genetica *121*, 107–118.

Chalkley, G.E., Moshkin, Y.M., Langenberg, K., Bezstarosti, K., Blastyak, A., Gyurkovics, H., Demmers, J.A.A., and Verrijzer, C.P. (2008). The Transcriptional Coactivator SAYP is a Trithorax Group Signature Subunit of the PBAP Chromatin Remodeling Complex. Mol. Cell. Biol. *28*, 2920–2929.

Collins, R.T., Furukawa, T., Tanese, N., and Treisman, J.E. (1999). Osa associates with the Brahma chromatin remodeling complex and promotes the activation of some target genes. EMBO J. *18*, 7029-7040.

Collins, R.T., and Treisman, J.E. (2000). Osa-containing Brahma chromatin remodeling complexes are required for the repression of Wingless target genes. Genes Dev. *14*, 3140–3152.

Davis, R.L. (1996). Physiology and biochemistry of Drosophila learning mutants. Physiol. Rev. *76*, 299-317.

Delgado-Morales, R., Agís-Balboa, R.C., Esteller, M., and Berdasco, M. (2017). Epigenetic mechanisms during ageing and neurogenesis as novel therapeutic avenues in human brain disorders. Clin. Epigenetics *9*, 67.

Di Donato, N., Rump, A., Koenig, R., Der Kaloustian, V.M., Halal, F., Sonntag, K., Krause, C., Hackmann, K., Hahn, G., Schrock, E., et al. (2014). Severe forms of Baraitser-Winter syndrome are caused by *ACTB* mutations rather than *ACTG1* mutations. Eur. J. Hum. Genet. *22*, 179–183.

Dias, C., Estruch, S.B., Graham, S.A., McRae, J., Sawiak, S.J., Hurst, J.A., Joss, S.K., Holder, S. E., Morton, J.E.V., Turner, C. et al. (2016). *BCL11A* Haploinsufficiency Causes an Intellectual Disability Syndrome and Dysregulates Transcription. Am. J. Hum. Genet. *99*, 253–274.

Dietzl, G., Chen, D., Schnorrer, F., Su, K.-C., Barinova, Y., Fellner, M., Gasser, B., Kinsey, K., Oppel, S., Scheiblauer, S., et al. (2007). A genome-wide transgenic RNAi library for conditional gene inactivation in *Drosophila*. Nature *448*, 151–156.

Dingwall, A.K., Beek, S.J., McCallum, C.M., Tamkun, J.W., Kalpana, G.V., Goff, S.P., and Scott, M.P. (1995). The *Drosophila* snrl and brm Proteins Are Related to Yeast SWI/SNF Proteins and Are Components of a Large Protein Complex. Mol. Biol. Cell *6*, 777–791.

Duffy, J.B. (2002). GAL4 System in *Drosophila*: A Fly Geneticist's Swiss Army Knife. Genesis *34*, 1–15.

Elfring, L.K., Daniel, C., Papoulas, O., Deuring, R., Sarte, M., Moseley, S., Beek, S.J., Waldrip, W.R., Daubresse, G., DePace, A., et al. (1998). Genetic Analysis of *brahma*: The Drosophila Homolog of the Yeast Chromatin Remodeling Factor SWI2/SNF2. Genetics *148*, 251-265.

Fire, A., Xu, S., Montgomery, M.K., Kostas, S.A., Driver, S.E., and Mello, C.C. (1998). Potent and specific genetic interference by double-stranded RNA in *Caenorhabditis elegans*. Nature *391*, 806–811.

Fish, M.P., Groth, A.C., Calos, M.P., and Nusse, R. (2007). Creating transgenic *Drosophila* by microinjecting the site-specific φC31 integrase mRNA and a transgene-containing donor plasmid. Nat. Protoc. *2*, 2325–2331.

Franz, M., Lopes, C.T., Huck, G., Dong, Y., Sumer, O., and Bader, G.D. (2015). Cytoscape.js: a graph theory library for visualisation and analysis. Bioinformatics *32*, 309–311.

Fuchs, E., and Flügge, G. (2014). Adult Neuroplasticity: More Than 40 Years of Research. Neural Plast. *2014*, 541870.

Gilissen, C., Hehir-Kwa, J.Y., Thung, D.T., van de Vorst, M., van Bon, B.W.M., Willemsen, M.H., Kwint, M., Janssen, I.M., Hoischen, A., Schenck, A., et al. (2014). Genome sequencing identifies major causes of severe intellectual disability. Nature *511*, 344–347.

Giordano, E., Rendina, R., Peluso, I., and Furia, M. (2002). RNAi Triggered by Symmetrically Transcribed Transgenes in *Drosophila melanogaster*. Genetics *160*, 637–648.

Goldberg, A.D., Allis, C.D., and Bernstein, E. (2007). Epigenetics: A Landscape Takes Shape. Cell *128*, 635–638.

Gramates, L.S., Marygold, S.J., dos Santos, G., Urbano, J.-M., Antonazzo, G., Matthews, B.B., Rey, A.J., Tabone, C.J., Crosby, M.A., Emmert, D.B., et al. (2017). FlyBase at 25: looking to the future. Nucleic Acids Res. *45*, D663-D671.

Green, E.W., Fedele, G., Giorgini, F., and Kyriacou, C.P. (2014). A *Drosophila* RNAi collection is subject to dominant phenotypic effects. Nat. Methods *11*, 222–223.

Gupta, S., Kim, S.Y., Artis, S., Molfese, D.L., Schumacher, A., Sweatt, J.D., Paylor, R.E., and Lubin, F.D. (2010). Histone Methylation Regulates Memory Formation. J. Neurosci. *30*, 3589–3599.

Hakim, Y., Yaniv, S.P., and Schuldiner, O. (2014). Astrocytes Play a Key Role in *Drosophila* Mushroom Body Axon Pruning. PLoS One *9*, e86178.

Harris, J.C. (2006). Intellectual Disability: Understanding its development, causes, classification, evaluation, and treatment. Oxford Univ. Press *35*, 42-98.

Havas, K., Flaus, A., Phelan, M., Kingston, R., Wade, P.A., Lilley, D.M.J., and Owen-Hughes, T. (2000). Generation of Superhelical Torsion by ATP-Dependent Chromatin Remodeling Activities. Cell *103*, 1133–1142.

Heisenberg, M. (1998). What Do The Mushroom Bodies Do For The Insect Brain? An Introduction. Learn. Mem. *5*, 1–10.

Herr, A., Mckenzie, L., Suryadinata, R., Sadowski, M., Parsons, L.M., Sarcevic, B., and Richardson, H.E. (2010). Geminin and Brahma act antagonistically to regulate EGFR-Ras-MAPK signaling in *Drosophila*. Dev. Biol. *344*, 36–51.

Ho, L., Ronan, J.L., Wu, J., Staahl, B.T., Chen, L., Kuo, A., Lessard, J., Nesvizhskii, A.I., Ranish, J., and Crabtree, G.R. (2009). An embryonic stem cell chromatin remodeling complex, esBAF, is essential for embryonic stem cell self-renewal and pluripotency. Proc. Natl. Acad. Sci. U.S.A *106*, 5181–5186.

Hoyer, J., Ekici, A.B., Endele, S., Popp, B., Zweier, C., Wiesener, A., Wohlleber, E., Dufke, A., Rossier, E., Petsch, C. et al. (2012). Haploinsufficiency of *ARID1B*, a Member of the SWI/SNF-A Chromatin-Remodeling Complex, Is a Frequent Cause of Intellectual Disability. Am. J. Hum. Genet. *90*, 565–572.

Hsieh, J., and Gage, F.H. (2005). Chromatin remodeling in neural development and plasticity. Curr. Opin. Cell Biol. *17*, 664–671.

Hu, Y., Flockhart, I., Vinayagam, A., Bergwitz, C., Berger, B., Perrimon, N., and Mohr, S.E. (2011). An integrative approach to ortholog prediction for disease-focused and other functional studies. BMC Bioinformatics *12*, 357.

Jenett, A., Rubin, G.M., Ngo, T.-T., Shepherd, D., Murphy, C., Dionne, H., Pfeiffer, B.D., Cavallaro, A., Hall, D., Jeter, J., et al. (2012). A GAL4-Driver Line Resource for *Drosophila* Neurobiology. Cell Rep. *2*, 991–1001.

Jennings, B.H. (2011). *Drosophila* - a versatile model in biology & medicine. Mater. Today *14*, 190–195.

Jiang, Y., Langley, B., Lubin, F.D., Renthal, W., Wood, M.A., Yasui, D.H., Kumar, A., Nestler, E.J., Akbarian, S., Beckel-Mitchener, A.C. (2008). Epigenetics in the Nervous System. J. Neurosci. *28*, 11753–11759.

Johnston, J.J., Wen, K.–K., Keppler-Noreuil, K., McKane, M., Maiers, J.L., Greiner, A., Sapp, J.C., NIH Intramural Sequencing Center, DeMali, K.A., Rubenstein, P.A., et al. (2013). Functional Analysis of a De Novo ACTB Mutation in a Patient with Atypical Baraitser-Winter Syndrome. Hum Mutat. *34*, 1242-1249.

Kadoch, C., and Crabtree, G.R. (2015). Mammalian SWI/SNF chromatin remodeling complexes and cancer: Mechanistic insights gained from human genomics. Sci. Adv. *1*, e1500447.

Kennison, J.A., and Tamkun, J.W. (1988). Dosage-dependent modifiers of Polycomb and Antennapedia mutations in *Drosophila*. Proc. Natl. Acad. Sci. U.S.A *85*, 8136–8140.

Kim, J.K., Huh, S.-O, Choi, H., Lee, K.-S, Shin, D., Lee, C., Nam, J.-S, Kim, H., Chung, H., Lee, H.W., et al. (2001). Srg3, a Mouse Homolog of Yeast *SWI3*, Is Essential for Early Embryogenesis and Involved in Brain Development. Mol. Cell Biol. *21*, 7787–7795.

Kishi, N., and Macklis, J.D. (2004). MECP2 is progressively expressed in post-migratory neurons and is involved in neuronal maturation rather than cell fate decisions. Mol. Cell Neurosci. *27*, 306-321.

Kleefstra, T., Schenck, A., Kramer, J.M., and van Bokhoven, H. (2014). The genetics of cognitive epigenetics. Neuropharm. *80*, 83–94.

Klochendler-Yievin, A., Fiette, L., Barra, J., Muchardt, J., Babinet, C., and Yaniv, M. (2000). The murine SNF5/INI1 chromatin remodeling factor is essential for embryonic development and tumor suppression. EMBO Rep. *1*, 500-506.

Kochinke, K., Zweier, C., Nijhof, B., Fenckova, M., Cizek, P., Honti, F., Keerthikumar, S., Oortveld, M.A.W., Kleefstra, T., Kramer, J.M., et al. (2016). Systematic Phenomics Analysis Deconvolutes Genes Mutated in Intellectual Disability into Biologically Coherent Modules. Am. J. Hum. Genet. *98*, 149–164.

Kramer, J.M., Kochinke, K., Oortveld, M.A.W., Marks, H., Kramer, D., de Jong, E.K., Asztalos, Z., Westwood, J.T., Stunnenberg, H.G., Sokolowski, M.B., et al. (2011). Epigenetic Regulation of Learning and Memory by *Drosophila* EHMT/G9a. PLoS Biol. *9*, e1000569.

Kurusu, M., Awasaki, T., Masuda-Nakagawa, L.M., Kawauchi, H., Ito, K., and Furukubo-Tokunaga, K. (2002). Embryonic and larval development of the

*Drosophila* mushroom bodies: concentric layer subdivisions and the role of *fasciclin II*. Development *129*, 409–419.

Lai, Y.-W., Chu, S.-Y., Wei, J.-Y., Cheng, C.-Y., Li, J.-C., Chen, P.-L., Chen, C.-H., and Yu, H.-H. (2016). *Drosophila* microRNA-34 Impairs Axon Pruning of Mushroom Body γ Neurons by Downregulating the Expression of Ecdysone Receptor. Sci. Rep. *6*, 39141.

Lam, G.T., Jiang, C., and Thummel, C.S. (1997). Coordination of larval and prepupal gene expression by the DHR3 orphan receptor during Drosophila metamorphosis. Development *124*, 1757–1769.

Lee, T., Lee, A., and Luo, L. (1999). Development of the Drosophila mushroom bodies: sequential generation of three distinct types of neurons from a neuroblast. Development *126*, 4065–4076.

Lee, T., Marticke, S., Sung, C., Robinow, S., and Luo, L. (2000). Cell-Autonomous Requirement of the USP/EcR-B Ecdysone Receptor for Mushroom Body Neuronal Remodeling in *Drosophila*. Neuron *28*, 807–818.

Lessard, J., Wu, J.I., Ranish, J.A., Wan, M., Winslow, M.M., Staahl, B.T., Wu, H., Aebersold, R., Graef, I.A., and Crabtree, G.R. (2007). An Essential Switch in Subunit Composition of a Chromatin Remodeling Complex during Neural Development. Neuron *55*, 201–215.

Levine, A.A., Guan, Z., Barco, A., Xu, S., Kandel, E.R., and Schwartz, J.H. (2005). CREB-binding protein controls response to cocaine by acetylating histones at the fosB promoter in the mouse striatum. Proc. Natl. Acad. Sci. U.S.A *102*, 19186–19191.

Luger, K., Mäder, A.W., Richmond, R.K., Sargent, D.F., and Richmond, T.J. (1997). Crystal structure of the nucleosome core particle at 2.8 Å resolution. Nature *389*, 251–260.

Luo, L., and O'Leary, D.D.M. (2005). Axon Retraction and Degeneration in Development and Disease. Annu. Rev. Neurosci. *28*, 127–156.

McIlwain, D.R., Berger, T., and Mak, T.W. (2013). Caspase Functions in Cell Death and Disease. Cold Spring Harb. Perspect. Biol. *5*, a008656.

Medvedeva, Y.A., Khamis, A.M., Kulakovskiy, I.V., Ba-Alawi, W., Bhuyan, M.S.I., Kawaji, H., Lassmann, T., Harbers, M., Forrest. A.R.R., Bajic, V.B., et al. (2014). Effects of cytosine methylation on transcription factor binding sites. BMC Genomics *15*, 119.

Miller, C.A., and Sweatt, J.D. (2007). Covalent Modification of DNA Regulates Memory Formation. Neuron *53*, 857–869.

Miller, C.A., Campbell, S.L., and Sweatt, J.D. (2008). DNA methylation and histone acetylation work in concert to regulate memory formation and synaptic plasticity. Neurobiol. Learn. Mem. *89*, 599–603.

Mitra, A.K., Dodge, J., Van Ness, J., Sokeye, I., and Van Ness, B. (2017). A de novo splice site mutation in EHMT1 resulting in Kleefstra syndrome with pharmacogenomics screening and behavior therapy for regressive behaviors. Mol. Genet. Genomic Med. *5*, 130–140.

Mohrmann, L., Langenberg, K., Krijgsveld, J., Kal, A.J., Heck, A.J.R., and Verrijzer, C.P. (2004). Differential Targeting of Two Distinct SWI/SNF-Related *Drosophila* Chromatin-Remodeling Complexes. Mol. Cell Biol. *24*, 3077–3088.

Morgan, T.H. (1910). Sex Limited Inheritance in Drosophila. Science *32*, 120–122.

Moshkin, Y.M., Mohrmann, L., van Ijcken, W.F.J., and Verrijzer, C.P. (2007). Functional Differentiation of SWI/SNF Remodelers in Transcription and Cell Cycle Control. Mol. Cell. Biol. *27*, 651–661.

Munno, D.W., and Syed, N.I. (2003). Synaptogenesis in the CNS: An Odyssey from Wiring Together to Firing Together. J. Physiol. *552*, 1–11.

Nan, X., Campoy, F.J., and Bird, A. (1997). MeCP2 Is a Transcriptional Repressor with Abundant Binding Sites in Genomic Chromatin. Cell *88*, 471–481.

Neigeborn, L., and Carlson, M. (1984). Genes Affecting the Regulation of *SUC2* Gene Expression by Glucose Repression in *Saccharomyces cerevisiae*. Genetics *108*, 845–858.

Ni, J.-Q., Liu, L.-P., Binari, R., Hardy, R., Shim, H.-S., Cavallaro, A., Booker, M., Pfeiffer, B.D., Markstein, M., Wang, H., et al. (2009). A Drosophila Resource of Transgenic RNAi Lines for Neurogenetics. Genetics *182*, 1089–1100.

Ni, J.-Q., Markstein, M., Binari, R., Pfeiffer, B., Liu, L.-P., Villalta, C., Booker, M., Perkins, L., and Perrimon, N. (2008). Vector and parameters for targeted transgenic RNA interference in *Drosophila melanogaster*. Nat. Methods *5*, 49–51.

Ni, J.-Q., Zhou, R., Czech, B., Liu, L.-P., Holderbaum, L., Yang-Zhou, D., Shim, H.-S., Tao, R., Handler, D., Karpowicz, P., et al. (2011). A genome-scale shRNA resource for transgenic RNAi in *Drosophila*. Nat. Methods *8*, 405–407.

Olave, I., Wang, W., Xue, Y., Kuo, A., and Crabtree, G.R. (2002). Identification of a polymorphic, neuron-specific chromatin remodeling complex. Genes Dev. *16*, 2509–2517.

Parrish, J.Z., Kim, M.D., Jan, L.Y., and Jan, Y.N. (2006). Genome-wide analyses identify transcription factors required for proper morphogenesis of *Drosophila* sensory neuron dendrites. Genes Dev. *20*, 820–835.

Perkins, L.A., Holderbaum, L., Tao, R., Hu, Y., Sopko, R., McCall, K., Yang-Zhou, D., Flockhart, I., Binari, R., Shim, H.-S., et al. (2015). The Transgenic RNAi Project at Harvard Medical School: Resources and Validation. Genetics *201*, 843–852.

Reiter, L.T., Potocki, L., Chien, S., Gribskov, M., and Bier, E. (2001). A Systematic Analysis of Human Disease-Associated Gene Sequences In *Drosophila melanogaster*. Genome Res. *11*, 1114–1125.

Rivière, J.-B., van Bon, B.W.M., Hoischen, A., Kholmanskikh, S.S., O'Roak, B.J., Gilissen, C., Gijsen, S., Sullivan, C.T., Christian, S.L., Abdul-Rahman, O.A., et al. (2012). *De novo* mutations in the actin genes *ACTB* and *ACTG1* cause Baraitser-Winter syndrome. Nat. Genet. *44*, 440-444.

Romero, O.A., and Sanchez-Cespedes, M. (2014). The SWI/SNF genetic blockade: effects in cell differentiation, cancer and developmental diseases. Oncogene *33*, 2681–2689.

Rudenko, A., and Tsai, L.-H. (2014). Epigenetic modifications in the nervous system and their impact upon cognitive impairments. Neuropharm. *80*, 70–82.

Santen, G.W.E., Aten, E., Sun, Y., Almomani, R., Gilissen, C., Nielsen, M., Kant, S.G., Snoeck, I.N., Peeters, E.A.J., Hilhorst-Hofstee, Y., et al. (2012). Mutations in SWI/SNF chromatin remodeling complex gene *ARID1B* cause Coffin-Siris syndrome. Nat. Genet. *44*, 379–380.

Santen, G.W.E., Aten, E., Vulto-van Silfhout, A.T., Pottinger, C., van Bon, B.W.M., van Minderhout, I.J.H.M., Snowdowne, R., van der Lans, C.A.C., Boogard, M., Linssen, M.M.L., et al. (2013). Coffin-Siris Syndrome and the BAF Complex: Genotype-Phenotype Study in 63 Patients. Hum. Mutat. *34*, 1519–1528.

Schindelin, J., Arganda-Carreras, I., Frise, E., Kaynig, V., Longair, M., Pietzsch, T., Preibisch, S., Rueden, C., Saalfeld, S., Schmid, B., et al. (2012). Fiji: an open source platform for biological-image analysis. Nat. Methods *9*, 676–682.

Schones, D.E, Cui, K., Cuddapah, S., Roh, T.-Y., Barski, A., Wang, Z., Wei, G., and Zhao, K. (2008). Dynamic Regulation of Nucleosome Positioning in the Human Genome. Cell *132*, 887–898.

Schubiger, M., Wade, A.A., Carney, G.E., Truman, J.W., and Bender, M. (1998). Drosophila EcR-B ecdysone receptor isoforms are required for larval molting and for neuron remodeling during metamorphosis. Development *125*, 2053–2062.

Schwaibold, E.M.C., Smogavec, M., Hobbiebrunken, E., Winter, L., Zoll, B., Burfeind, P., Brockmann, K., and Pauli, S. (2014). Intragenic duplication of *EHMT1* gene results in Kleefstra syndrome. Mol. Cytogenet. *7*, 74.

Smrt, R.D., Eaves-Egenes, J., Barkho, B.Z., Santistevan, N.J., Zhao, C., Aimone, J.B., Gage, F.H., and Zhao, X. (2007). Mecp2 deficiency leads to delayed maturation and altered gene expression in hippocampal neurons. Neurobiol. Dis. *27*, 77-89.

Son, E.Y., and Crabtree, G.R. (2014). The role of BAF (mSWI/SNF) complexes in mammalian neural development. Am. J. Med. Genet. C. Semin. Med. Genet. *166*, 333-349.

Stephenson, R., and Metcalfe, N.H. (2013). *Drosophila melanogaster*: a fly through its history and current use. J. R. Coll. Physicians Edinb. *43*, 70–5.

Stern, M., Jensen, R., and Herskowitz, I. (1984). Five *SWI* genes are required for expression of the *HO* gene in yeast. J. Mol. Biol. *178*, 853–868.

Sweatt, J.D. (2013). The Emerging Field of Neuroepigenetics. Neuron *80*, 624–632.

Tea, J.S., and Luo, L. (2011). The chromatin remodeling factor Bap55 functions through the TIP60 complex to regulate olfactory projection neuron dendrite targeting. Neural Dev. *6*, 5.

Tsurusaki, Y., Okamoto, N., Ohashi, H., Kosho, T., Imai, Y., Hibi-Ko, Y., Kaname, T., Naritomi, K., Kawame, H., Wakui, K. et al. (2012). Mutations affecting components of the SWI/SNF complex cause Coffin-Siris syndrome. Nat. Genet. *44*, 376–378.

Vaillend, C., Poirier, R., and Laroche, S. (2008). Genes, plasticity and mental retardation. Behav. Brain Res. *192*, 88–105.

van Bokhoven, H., and Kramer, J.M. (2010). Disruption of the epigenetic code: An emerging mechanism in mental retardation. Neurobiol. Dis. *39*, 3–12.

Van Houdt, J.K.J., Nowakowska, B.A., Sousa, S.B., van Schaik, B.D.C., Seuntjens, E., Avonce, N., Sifrim, A., Abdul-Rahman, O.A., van den Boogard, M.–J.H., Bottani, A., et al. (2012). Heterozygous missense mutations in *SMARCA2* cause Nicolaides-Baraitser syndrome. Nat. Genet. *44*, 445–449.

Venken, K.J.T., and Bellen, H.J. (2005). Emerging technologies for gene manipulation in *Drosophila melanogaster*. Nat. Rev. Genet. *6*, 167–178.

Vignali, M., Hassan, A.H., Neely, K.E., and Workman, J.L. (2000). ATP-Dependent Chromatin-Remodeling Complexes. Mol. Cell Biol. *20*, 1899–1910.

Vissers, L.E.L.M., de Ligt, J., Gilissen, C., Janssen, I., Steehouwer, M., de Vries, P., van Lier, B., Arts, P., Wieskamp, N., del Rosario, M., et al. (2010). A *de novo* paradigm for mental retardation. Nat. Genet. *42*, 1109–1112.

Vissers, L.E.L.M., Gilissen, C., and Veltman, J.A. (2016). Genetic studies in intellectual disability and related disorders. Nat. Rev. Genet. *17*, 9–18.

Vogel-Ciernia, A., Kramár, E.A., Matheos, D.P., Havekes, R., Hemstedt, T.J., Magnan, C.N., Sakata, K., Tran, A., Azzawi, S., Lopez, A., et al. (2017). Mutation of neuron-specific chromatin remodeling subunit BAF53b: rescue of plasticity and memory by manipulating actin remodeling. Learn. Mem. *24*, 199–209.

Vogel-Ciernia, A., Matheos, D.P., Barrett, R.M., Kramár, E.A., Azzawi, S., Chen, Y., Magnan, C.N., Zeller, M., Sylvain, A., Haettig, J., et al. (2013). The Neuron-specific Chromatin Regulatory Subunit BAF53b is Necessary for Synaptic Plasticity and Memory. Nat. Neurosci. *16*, 552–561.

Vorobyeva, N.E., Nikolenko, J.V., Krasnov, A.N., Kuzmina, J.L., Panov, V.V., Nabirochkina, E.N., Georgieva, S.G., and Shidlovskii, Y.V. (2011). SAYP interacts with DHR3 nuclear receptor and participates in ecdysone-dependent transcription regulation. Cell Cycle *10*, 1821–1827.

Vorobyeva, N.E., Nikolenko, J.V., Nabirochkina, E.N., Krasnov, A.N., Shidlovskii, Y.V., and Georgieva, S.G. (2012). SAYP and Brahma are important for 'repressive' and 'transient' Pol II pausing. Nucleic Acids Res. *40*, 7319–7331.

Waddington, C.H. (2012). The Epigenotype. Int. J. Epidemiol. *41*, 10–13.

Weaver, I.C.G., Cervoni, N., Champagne, F.A., D'Alessio, A.C., Sharma, S., Seckl, J.R., Dymov, S., Szyf, M., and Meaney, M.J. (2004). Epigenetic programming by maternal behavior. Nat. Neurosci. *7*, 847–854.

Whitehouse, I., Flaus, A., Cairns, B.R., White, M.F., Workman, J.L., and Owen-Hughes, T. (1999). Nucleosome mobilization catalysed by the yeast SWI/SNF complex. Nature *400*, 784–787.

Wieczorek, D., Bögershausen, N., Beleggia, F., Steiner-Haldenstätt, S., Pohl, E., Li, Y., Milz, E., Martin, M., Thiele, H., Altmüller, J., et al. (2013). A comprehensive molecular study on Coffin-Siris and Nicolaides-Baraitser syndromes identifies a broad molecular and clinical spectrum converging on altered chromatin remodeling. Hum. Mol. Genet. *22*, 5121–5135.

Wolff, D., Endele, S., Azzarello-Burri, S., Hoyer, J., Zweier, M., Schanze, I., Schmitt, B., Rauch, A., Reis, A., and Zweier, C. (2012). In-Frame Deletion and Missense Mutations of the C-Terminal Helicase Domain of *SMARCA2* in Three Patients with Nicolaides-Baraitser Syndrome. Mol. Syndromol. *2*, 237–244.

Wu, J.I., Lessard, J., Olave, I.A., Qiu, Z., Ghosh, A., Graef, I.A., and Crabtree, G.R. (2007). Regulation of Dendritic Development by Neuron-Specific Chromatin Remodeling Complexes. Neuron *56*, 94–108.

Yao, T.-P., Forman, B.M., Jiang, Z., Cherbas, L., Chen, J.-D., McKeown, M., Cherbas, P., and Evans, R.M. (1993). Functional ecdysone receptor is the product of *EcR* and *Ultraspiracle* genes. Nature *366*, 476–479.

Yoo, A.S., and Crabtree, G.R. (2009). ATP-dependent chromatin remodeling in neural development. Curr. Opin. Neurobiol. *19*, 120–126.

Yoo, A.S., Staahl, B.T., Chen, L., and Crabtree, G.R. (2009). MicroRNA-mediated switching of chromatin-remodeling complexes in neural development. Nature *460*, 642–646.

Zhang, Y., Smith, C.L., Saha, A., Grill, S.W., Mihardja, S., Smith, S.B., Cairns, B.R., Peterson, C.L., and Bustamante, C. (2006). DNA Translocation and Loop Formation Mechanism of Chromatin Remodeling by SWI/SNF and RSC. Mol. Cell *24*, 559–568.

Zheng, X., Wang, J., Haerry, T.E., Wu, A.Y.-H., Martin, J., O'Connor, M.B., Lee, C.-H.J., and Lee, T. (2003). TGF-β Signaling Activates Steroid Hormone Receptor Expression during Neuronal Remodeling in the *Drosophila* Brain. Cell *112*, 303–315.

Zhou, Z., Hong, E.J., Cohen, S., Zhao, W.-N., Ho, H.H., Schmidt, L., Chen, W.G., Lin, Y., Savner, E., Griffith, E.C., et al. (2006). Brain-Specific Phosphorylation of MeCP2 Regulates Activity-Dependent *Bdnf* Transcription, Dendritic Growth, and Spine Maturation. Neuron *52*, 255–269.

Zraly, C.B., Marenda, D.R., Nanchal, R., Cavalli, G., Muchardt, C., and Dingwall, A.K. (2003). SNR1 is an essential subunit in a subset of *Drosophila* brm complexes, targeting specific functions during development. Dev. Biol. *253*, 291–308.

Zraly, C.B., Middleton, F.A., and Dingwall, A.K. (2006). Hormone-response genes are direct *in vivo* regulatory targets of Brahma (SWI/SNF) complex function. J. Biol. Chem. *281*, 35305–35315.

Zwarts, L., Vanden Broeck, L., Cappuyns, E., Ayroles, J.F., Magwire, M.M., Vulsteke, V., Clements, J., Mackay, T.F.C., and Callaerts, P. (2015). The genetic basis of

natural variation in mushroom body size in *Drosophila melanogaster*. Nat. Commun. *6*, 10115.

# 6   APPENDICES

**Appendix A: Fly stocks used in this M.Sc. thesis.**

| Driver Lines and Controls | | | |
|---|---|---|---|
| **Stock #** | **Genotype** | **Source** | **Description** |
| 48667 | *w$^{1118}$; P{GMR14H06-GAL4}attP2* | BDSC | *R14H06-GAL4*: Expresses GAL4 at or near *rutabaga* (FGgn0003301) |
| 5137 | *y$^1$w$^*$; P{UAS-mCD8::GFP.L}LL5, P{UAS-mCD8::GFP.L}2* | BDSC | *UAS-GFP*: Expresses GFP under UAS control |
| 5130 | *y$^1$ w$^*$; Pin$^{Yt}$/CyO; P{UAS-mCD8::GFP.L}LL6* | BDSC | *UAS-GFP*: Expresses GFP under UAS control |
| 24650 | *w$^{1118}$; P{UAS-Dcr-2.D}2* | BDSC | *UAS-Dicer-2*: Expresses Dicer-2 under UAS control |
| 25374 | *y$^1$ w$^*$; P{Act5C-GAL4-w}E1/CyO* | BDSC | *Act5c-GAL4*: Expresses GAL4 ubiquitously under control of the Act5C promoter |
| MB607B | *{R19B03-p65ADZp}attP40; R39A11-39A11_ZpGAL4DBD} attP2* | Janelia Fly Light | Split-GAL4: Expresses GAL4 specifically in 75 neurons within the dorsal portion of the MB γ lobe |
| **Control Stocks** | | | |
| 35785 | *y$^1$sc$^*$v$^1$; P{VALIUM20-mCherry}attP2* | BDSC | mCherry-RNAi: RNA hairpin targeting mCherry |
| 36303 | *y$^1$ v$^1$; P{CaryP}attP2* | BDSC | *attP2* genetic background control |
| 36304 | *y$^1$ v$^1$; P{CaryP}attP40* | BDSC | *attP40* genetic background control |
| 60 000 | *w$^{1118}$* | BDSC | Isogenic host strain for the GD genetic library |
| 60 100 | *y,w$^{1118}$;P{attP,y[ +],w[3`]}* | BDSC | Isogenic host strain for the KK genetic library |
| **Inducible RNAi Stocks** | | | |
| **Stock #** | **Genotype** | **Source** | **Description** |
| 42651 | *y$^1$ sc$^*$ v$^1$; P{TRiP.HMS02487}attP2* | BDSC | *UAS-RNAi* against *Act5C* |
| 101438 | *P{KK109161}VIE-260B* | VDRC | *UAS-RNAi* against *Act5C* |
| 26308 | *y$^1$ v$^1$; P{TRiP.JF02080}attP2* | BDSC | *UAS-RNAi* against *Bap170* |
| 34582 | *w$^{1118}$; P{GD10922}v34582/TM3* | VDRC | *UAS-RNAi* against *Bap170* |

| 24703 | $w^{1118}$; P{GD11955}v24703/CyO | VDRC | UAS-RNAi against Bap55 |
|---|---|---|---|
| 31708 | $y^1$ $v^1$; P{TRiP.HM04015}attP2/TM3, Sb$^1$ | BDSC | UAS-RNAi against Bap55 |
| 32503 | $y^1$ sc$^*$ $v^1$; P{TRiP.HMS00507}attP2 | BDSC | UAS-RNAi against Bap60 |
| 33954 | $y^1$ sc$^*$ $v^1$; P{TRiP.HMS00909}attP2 | BDSC | UAS-RNAi against Bap60 |
| 35714 | $y^1$ sc$^*$ $v^1$; P{TRiP.GLV21079}attP2 | BDSC | UAS-RNAi against BCL7-like |
| 20410 | $w^{1118}$; P{GD9322}v20410 | VDRC | UAS-RNAi against BCL7-like |
| 37720 | $w^{1118}$; P{GD4507}v37720 | VDRC | UAS-RNAi against brm |
| 34520 | $y^1$ sc* $v^1$; P{TRiP.HMS00050}attP2 | BDSC | UAS-RNAi against brm |
| 31712 | $y^1$ $v^1$; P{TRiP.HM04019}attP2 | BDSC | UAS-RNAi against brm |
| 50606 | $y^1$ sc$^*$ $v^1$; P{TRiP.HMC02408}attP2 | BDSC | UAS-RNAi against CG10555 |
| 105802 | P{KK111183}VIE-260B | VDRC | UAS-RNAi against CG10555 |
| 37670 | $w^{1118}$; P{GD4426}v37670 | VDRC | UAS-RNAi against CG7154 |
| 107992 | P{KK100498}VIE-260B | VDRC | UAS-RNAi against CG7154 |
| 23170 | $w^{1118}$; P{GD13222}v23170 | VDRC | UAS-RNAi against CG9650 |
| 40852 | $y^1$ $v^1$; P{TRiP.HMS02019}attP40 | BDSC | UAS-RNAi against CG9650 |
| 104402 | P{KK108364}VIE-260B | VDRC | UAS-RNAi against CG9650 |
| 26218 | $y^1$ $v^1$; P{TRiP.JF02116}attP2 | BDSC | UAS-RNAi against Bap111 |
| 35242 | $y^1$ sc$^*$ $v^1$; P{TRiP.GL00129}attP2 | BDSC | UAS-RNAi against Bap111 |
| 32346 | $y^1$ sc$^*$ $v^1$; P{TRiP.HMS00337}attP2 | BDSC | UAS-RNAi against e(y)3 |
| 105946 | P{KK112108}VIE-260B | VDRC | UAS-RNAi against e(y)3 |
| 110712 | P{KK102003}VIE-260B | VDRC | UAS-RNAi against mor |
| 6969 | $w^{1118}$; P{GD1257}v6969 | VDRC | UAS-RNAi against mor |
| 38285 | $y^1$ sc$^*$ $v^1$; P{TRiP.HMS01738}attP40 | BDSC | UAS-RNAi against osa |
| 7810 | $w^{1118}$; P{GD1502}v7810 | VDRC | UAS-RNAi against osa |
| 32840 | $y^1$ sc$^*$ $v^1$; P{TRiP.HMS00531}attP2 | BDSC | UAS-RNAi against polybromo |
| 108618 | P{KK101808}VIE-260B | VDRC | UAS-RNAi against polybromo |
| 32372 | $y^1$ sc$^*$ $v^1$; P{TRiP.HMS00363}attP2 | BDSC | UAS-RNAi against Snr1 |
| 12644 | $w^{1118}$; P{GD4140}v12644 | VDRC | UAS-RNAi against Snr1 |

**Appendix B: Genetic background controls for the RNAi lines used in this study.**

| Gene | Stock # | Source | Insertion Site | Control |
|---|---|---|---|---|
| *CG9650* | 40852 | VALIUM20 | Chromosome 2 | *attP40* (36304) |
| *osa* | 38285 | VALIUM20 | Chromosome 2 | *attP40* (36304) |
| *Bap170* | 34582 | GD | Chromosome 3 | GD (60 000) |
| *Bap55* | 24703 | GD | Chromosome 2 | GD (60 000) |
| *BCL7-like* | 20410 | GD | Chromosome 3 | GD (60 000) |
| *brm* | 37720 | GD | Chromosome 3 | GD (60 000) |
| *CG7154* | 37670 | GD | Chromosome 2 | GD (60 000) |
| *CG9650* | 23170 | GD | Chromosome 2 | GD (60 000) |
| *mor* | 6969 | GD | Chromosome 3 | GD (60 000) |
| *osa* | 7810 | GD | Chromosome 3 | GD (60 000) |
| *Snr1* | 12644 | GD | Chromosome 2 | GD (60 000) |
| *Act5C* | 101438 | KK | Chromosome 2 | KK (60 100) |
| *CG10555* | 105802 | KK | Chromosome 2 | KK (60 100) |
| *CG7154* | 107992 | KK | Chromosome 2 | KK (60 100) |
| *CG9650* | 104402 | KK | Chromosome 2 | KK (60 100) |
| *mor* | 110712 | KK | Chromosome 2 | KK (60 100) |
| *e(y)3* | 105946 | KK | Chromosome 2 | KK (60 100) |
| *polybromo* | 108618 | KK | Chromosome 2 | KK (60 100) |
| *Snr1* | 32372 | VALIUM20 | Chromosome 3 | mCherry (35785) |
| *polybromo* | 32840 | VALIUM20 | Chromosome 3 | mCherry (35785) |
| *e(y)3* | 32346 | VALIUM20 | Chromosome 3 | mCherry (35785) |
| *Bap60* | 33954 | VALIUM20 | Chromosome 3 | mCherry (35785) |
| *Bap60* | 32503 | VALIUM20 | Chromosome 3 | mCherry (35785) |
| *Act5C* | 42651 | VALIUM20 | Chromosome 3 | mCherry (35785) |
| *brm* | 34520 | VALIUM20 | Chromosome 3 | mCherry (35785) |
| *Bap111* | 35242 | VALIUM22 | Chromosome 3 | mCherry (35785) |
| *CG10555* | 50606 | VALIUM20 | Chromosome 3 | mCherry (35785) |
| *BCL7-like* | 35714 | VALIUM21 | Chromosome 3 | mCherry (35785) |
| *Bap111* | 26218 | VALIUM10 | Chromosome 3 | *UAS-Dcr-2*, mCherry, (35785) |
| *Bap55* | 31708 | VALIUM1 | Chromosome 3 | *UAS-Dcr-2*, mCherry, (35785) |
| *brm* | 31712 | VALIUM1 | Chromosome 3 | *UAS-Dcr-2*, mCherry, (35785) |
| *Bap170* | 26308 | VALIUM10 | Chromosome 3 | *UAS-Dcr-2*, mCherry, (35785) |

SWI/SNF knockdowns were compared to their appropriate genetic background control using a two-tailed Fishers exact test.

**Appendix C: Analysis of gross mushroom body morphology following SWI/SNF knockdown.**

| Gene | Stock # | Brain # | Missing α (%) | Missing β (%) | B-lobe crossover (%) | | Extra dorsal projections (%) | | Stunted γ-lobes (%) | |
|---|---|---|---|---|---|---|---|---|---|---|
| Controls | 36303 | 12 | 0 | 0 | Normal | 75 | Normal | 91.67 | Normal | 100 |
| | | | | | Mild | 8.33 | Mild | 8.33 | Mild | 0 |
| | | | | | Moderate | 16.67 | Moderate | 0 | Moderate | 0 |
| | | | | | Severe | 0 | Severe | 0 | Severe | 0 |
| | Dcr-2, 36303 | 6 | 0 | 0 | Normal | 83.33 | Normal | 100 | Normal | 100 |
| | | | | | Mild | 16.67 | Mild | 0 | Mild | 0 |
| | | | | | Moderate | 0 | Moderate | 0 | Moderate | 0 |
| | | | | | Severe | 0 | Severe | 0 | Severe | 0 |
| | 35785 | 17 | 0 | 5.88 | Normal | 88.24 | Normal | 58.82 | Normal | 100 |
| | | | | | Mild | 11.76 | Mild | 41.18 | Mild | 0 |
| | | | | | Moderate | 0 | Moderate | 0 | Moderate | 0 |
| | | | | | Severe | 0 | Severe | 0 | Severe | 0 |
| | Dcr-2, 35785 | 7 | 0 | 0 | Normal | 100 | Normal | 71.43 | Normal | 100 |
| | | | | | Mild | 0 | Mild | 28.57 | Mild | 0 |
| | | | | | Moderate | 0 | Moderate | 0 | Moderate | 0 |
| | | | | | Severe | 0 | Severe | 0 | Severe | 0 |
| | 36304 | 21 | 0 | 0 | Normal | 80.95 | Normal | 85.71 | Normal | 100 |
| | | | | | Mild | 9.52 | Mild | 14.29 | Mild | 0 |
| | | | | | Moderate | 9.52 | Moderate | 0 | Moderate | 0 |
| | | | | | Severe | 0 | Severe | 0 | Severe | 0 |
| | 60 000 | 23 | 0 | 0 | Normal | 95.65 | Normal | 100 | Normal | 100 |
| | | | | | Mild | 4.35 | Mild | 0 | Mild | 0 |
| | | | | | Moderate | 0 | Moderate | 0 | Moderate | 0 |
| | | | | | Severe | 0 | Severe | 0 | Severe | 0 |
| | 60 100 | 25 | 8 | 0 | Normal | 88 | Normal | 100 | Normal | 100 |

| | | | | | | | | | | |
|---|---|---|---|---|---|---|---|---|---|---|
| | | | | | Mild | 4 | Mild | 0 | Mild | 0 |
| | | | | | Moderate | 8 | Moderate | 0 | Moderate | 0 |
| | | | | | Severe | 0 | Severe | 0 | Severe | 0 |
| *brm* | 37720 | 10 | 0 | 0 | Normal | 60 | Normal | 100 | Normal | 100 |
| | | | | | Mild | 10 | Mild | 0 | Mild | 0 |
| | | | | | Moderate | 30 | Moderate | 0 | Moderate | 0 |
| | | | | | Severe | 0 | Severe | 0 | Severe | 0 |
| | 31712 | 10 | 0 | 0 | Normal | 80 | Normal | 100 | Normal | 100 |
| | | | | | Mild | 10 | Mild | 0 | Mild | 0 |
| | | | | | Moderate | 10 | Moderate | 0 | Moderate | 0 |
| | | | | | Severe | 0 | Severe | 0 | Severe | 0 |
| *Bap60* | 32503 | 16 | 0 | 6.25 | Normal | 93.75 | Normal | 0 | Normal | 68.75 |
| | | | | | Mild | 0 | Mild | 18.75 | Mild | 31.25 |
| | | | | | Moderate | 6.25 | Moderate | 56.25 | Moderate | 0 |
| | | | | | Severe | 0 | Severe | 25 | Severe | 0 |
| | 33954 | 20 | 0 | 0 | Normal | 35 | Normal | 0 | Normal | 0 |
| | | | | | Mild | 25 | Mild | 0 | Mild | 5 |
| | | | | | Moderate | 30 | Moderate | 40 | Moderate | 40 |
| | | | | | Severe | 10 | Severe | 60 | Severe | 55 |
| *Act5C* | 42651 | 12 | 8.33 | 0 | Normal | 91.67 | Normal | 8.33 | Normal | 0 |
| | | | | | Mild | 0 | Mild | 66.67 | Mild | 50 |
| | | | | | Moderate | 8.33 | Moderate | 8.33 | Moderate | 25 |
| | | | | | Severe | 0 | Severe | 16.67 | Severe | 25 |
| | 101438 | 20 | 0 | 0 | Normal | 95 | Normal | 0 | Normal | 0 |
| | | | | | Mild | 0 | Mild | 10 | Mild | 20 |
| | | | | | Moderate | 5 | Moderate | 20 | Moderate | 65 |
| | | | | | Severe | 0 | Severe | 70 | Severe | 15 |
| *Snr1* | 32372 | 15 | 0 | 0 | Normal | 93.33 | Normal | 6.67 | Normal | 6.67 |

| | | | | | | | | | | |
|---|---|---|---|---|---|---|---|---|---|---|
| | | | | | **Mild** | 6.67 | **Mild** | 13.33 | **Mild** | 13.33 |
| | | | | | **Moderate** | 0 | **Moderate** | 66.67 | **Moderate** | 66.67 |
| | | | | | **Severe** | 0 | **Severe** | 13.33 | **Severe** | 13.33 |
| | 12644 | 14 | 0 | 7.14 | **Normal** | 85.71 | **Normal** | 100 | **Normal** | 100 |
| | | | | | **Mild** | 0 | **Mild** | 0 | **Mild** | 0 |
| | | | | | **Moderate** | 14.29 | **Moderate** | 0 | **Moderate** | 0 |
| | | | | | **Severe** | 0 | **Severe** | 0 | **Severe** | 0 |
| *mor* | 6969 | 7 | 0 | 0 | **Normal** | 71.43 | **Normal** | 100 | **Normal** | 100 |
| | | | | | **Mild** | 14.29 | **Mild** | 0 | **Mild** | 0 |
| | | | | | **Moderate** | 14.29 | **Moderate** | 0 | **Moderate** | 0 |
| | | | | | **Severe** | 0 | **Severe** | 0 | **Severe** | 0 |
| | 110712 | 19 | 0 | 0 | **Normal** | 84.21 | **Normal** | 100 | **Normal** | 100 |
| | | | | | **Mild** | 15.79 | **Mild** | 0 | **Mild** | 0 |
| | | | | | **Moderate** | 0 | **Moderate** | 0 | **Moderate** | 0 |
| | | | | | **Severe** | 0 | **Severe** | 0 | **Severe** | 0 |
| *Bap55* | 24703 | 18 | 0 | 5.56 | **Normal** | 94.44 | **Normal** | 83.33 | **Normal** | 100 |
| | | | | | **Mild** | 0 | **Mild** | 11.11 | **Mild** | 0 |
| | | | | | **Moderate** | 5.56 | **Moderate** | 5.56 | **Moderate** | 0 |
| | | | | | **Severe** | 0 | **Severe** | 0 | **Severe** | 0 |
| *Bap111* | 26218 | 21 | 4.76 | 0 | **Normal** | 85.71 | **Normal** | 100 | **Normal** | 95.24 |
| | | | | | **Mild** | 9.52 | **Mild** | 0 | **Mild** | 4.76 |
| | | | | | **Moderate** | 4.76 | **Moderate** | 0 | **Moderate** | 0 |
| | | | | | **Severe** | 0 | **Severe** | 0 | **Severe** | 0 |
| | 35242 | 11 | 0 | 0 | **Normal** | 81.82 | **Normal** | 100 | **Normal** | 100 |
| | | | | | **Mild** | 9.09 | **Mild** | 0 | **Mild** | 0 |
| | | | | | **Moderate** | 9.09 | **Moderate** | 0 | **Moderate** | 0 |

| Gene | ID | | | | | | | | | |
|---|---|---|---|---|---|---|---|---|---|---|
| | | | | | Severe | 0 | Severe | 0 | Severe | 0 |
| *CG9650* | 40852 | 25 | 0 | 0 | Normal | 96 | Normal | 0 | Normal | 100 |
| | | | | | Mild | 0 | Mild | 0 | Mild | 0 |
| | | | | | Moderate | 4 | Moderate | 28 | Moderate | 0 |
| | | | | | Severe | 0 | Severe | 72 | Severe | 0 |
| | 23170 | 20 | 0 | 0 | Normal | 80 | Normal | 100 | Normal | 100 |
| | | | | | Mild | 5 | Mild | 0 | Mild | 0 |
| | | | | | Moderate | 15 | Moderate | 0 | Moderate | 0 |
| | | | | | Severe | 0 | Severe | 0 | Severe | 0 |
| | 104402 | 14 | 7.14 | 0 | Normal | 92.86 | Normal | 78.57 | Normal | 100 |
| | | | | | Mild | 0 | Mild | 14.29 | Mild | 0 |
| | | | | | Moderate | 7.14 | Moderate | 7.14 | Moderate | 0 |
| | | | | | Severe | 0 | Severe | 0 | Severe | 0 |
| *CG7154* | 37670 | 22 | 4.55 | 0 | Normal | 72.73 | Normal | 77.27 | Normal | 100 |
| | | | | | Mild | 4.55 | Mild | 22.73 | Mild | 0 |
| | | | | | Moderate | 22.73 | Moderate | 0 | Moderate | 0 |
| | | | | | Severe | 0 | Severe | 0 | Severe | 0 |
| | 107992 | 16 | 6.25 | 6.25 | Normal | 87.50 | Normal | 6.25 | Normal | 100 |
| | | | | | Mild | 6.25 | Mild | 18.75 | Mild | 0 |
| | | | | | Moderate | 6.25 | Moderate | 25 | Moderate | 0 |
| | | | | | Severe | 0 | Severe | 50 | Severe | 0 |
| *CG10555* | 105802 | 25 | 12 | 12 | Normal | 92 | Normal | 72 | Normal | 84 |
| | | | | | Mild | 0 | Mild | 16 | Mild | 12 |
| | | | | | Moderate | 8 | Moderate | 8 | Moderate | 4 |
| | | | | | Severe | 0 | Severe | 4 | Severe | 0 |
| *BCL7-like* | 20410 | 16 | 6.25 | 6.25 | Normal | 100 | Normal | 93.75 | Normal | 93.75 |
| | | | | | Mild | 0 | Mild | 0 | Mild | 0 |
| | | | | | Moderate | 0 | Moderate | 6.25 | Moderate | 6.25 |
| | | | | | Severe | 0 | Severe | 0 | Severe | 0 |

| Gene | | | | | | | | | | |
|---|---|---|---|---|---|---|---|---|---|---|
| *osa* | 7810 | 15 | 0 | 6.67 | **Normal** | 93.33 | **Normal** | 100 | **Normal** | 93.33 |
| | | | | | **Mild** | 6.67 | **Mild** | 0 | **Mild** | 0 |
| | | | | | **Moderate** | 0 | **Moderate** | 0 | **Moderate** | 6.67 |
| | | | | | **Severe** | 0 | **Severe** | 0 | **Severe** | 0 |
| | 38285 | 20 | 0 | 0 | **Normal** | 45 | **Normal** | 90 | **Normal** | 85 |
| | | | | | **Mild** | 20 | **Mild** | 5 | **Mild** | 5 |
| | | | | | **Moderate** | 20 | **Moderate** | 5 | **Moderate** | 5 |
| | | | | | **Severe** | 15 | **Severe** | 0 | **Severe** | 5 |
| *polybromo* | 32840 | 14 | 0 | 7.14 | **Normal** | 100 | **Normal** | 100 | **Normal** | 100 |
| | | | | | **Mild** | 0 | **Mild** | 0 | **Mild** | 0 |
| | | | | | **Moderate** | 0 | **Moderate** | 0 | **Moderate** | 0 |
| | | | | | **Severe** | 0 | **Severe** | 0 | **Severe** | 0 |
| | 108618 | 11 | 0 | 9.09 | **Normal** | 100 | **Normal** | 100 | **Normal** | 100 |
| | | | | | **Mild** | 0 | **Mild** | 0 | **Mild** | 0 |
| | | | | | **Moderate** | 0 | **Moderate** | 0 | **Moderate** | 0 |
| | | | | | **Severe** | 0 | **Severe** | 0 | **Severe** | 0 |
| *e(y)3* | 32346 | 30 | 0 | 0 | **Normal** | 90 | **Normal** | 10 | **Normal** | 100 |
| | | | | | **Mild** | 0 | **Mild** | 13.33 | **Mild** | 0 |
| | | | | | **Moderate** | 10 | **Moderate** | 23.33 | **Moderate** | 0 |
| | | | | | **Severe** | 0 | **Severe** | 53.33 | **Severe** | 0 |
| | 105946 | 16 | 0 | 0 | **Normal** | 100 | **Normal** | 0 | **Normal** | 87.5 |

| | | | | | | | | | | |
|---|---|---|---|---|---|---|---|---|---|---|
| | | | | | | | | | | 0 |
| | | | | | Mild | 0 | Mild | 50 | Mild | 0 |
| | | | | | Moderate | 0 | Moderate | 43.75 | Moderate | 12.50 |
| | | | | | Severe | 0 | Severe | 6.25 | Severe | 0 |
| *Bap170* | 26308 | 31 | 0 | 6.45 | Normal | 96.77 | Normal | 87.10 | Normal | 87.10 |
| | | | | | Mild | 3.23 | Mild | 6.45 | Mild | 6.45 |
| | | | | | Moderate | 0 | Moderate | 6.45 | Moderate | 6.45 |
| | | | | | Severe | 0 | Severe | 0 | Severe | 0 |
| | 34582 | 12 | 8.33 | 8.33 | Normal | 50 | Normal | 91.67 | Normal | 100 |
| | | | | | Mild | 25 | Mild | 0 | Mild | 0 |
| | | | | | Moderate | 25 | Moderate | 0 | Moderate | 0 |
| | | | | | Severe | 0 | Severe | 8.33 | Severe | 0 |

# 7    CURRICULUM VITAE

# Melissa Christine Chubak

## POST-SECONDARY EDUCATION:

**Western University, London, ON, Canada**                                                    **2015-2017**
- M.Sc., Biology (Collaborative Program in Developmental Biology)

**Western University, London, ON, Canada**                                                    **2011-2015**
- B.Sc., Honours Specialization in Genetics

## CONFERENCE POSTER PRESENTATIONS:

**Chubak, M.C.,** and Kramer, J.M. The SWI/SNF complex is required for neuronal γ-lobe remodelling in the *Drosophila* mushroom body. Canadian *Drosophila* Research Conference. Banff, AB, Canada. June, 2017.

**Chubak, M.C.,** and Kramer, J.M. The SWI/SNF complex is required for axon morphogenesis in the *Drosophila* mushroom body. The 3$^{rd}$ Canadian Conference on Epigenetics. Esterel, QC, Canada. September, 2016.

## PUBLICATIONS:

Koemans, T.S., Kleefstra, T., **Chubak, M.C.,** Stone., M.H., Reijnders, M.R.F., de Munnik, S., Willemsen, M.H., Fenckoya, M., Stumpel, C.T.R.M., Bok, L.A., et al. Functional convergence of histone methyltransferases EHMT1 and KMT2C involved in intellectual disability and autism spectrum disorder. PLoS Genetics (accepted).

## AWARDS:

**Western University, London, ON, Canada**                                                    **2015-2017**
- Western Graduate Research Scholarship

**Western University, London, ON, Canada**                                                    **2017**
- Department of Biology Travel Award

**Children's Health Research Institute, London, ON, Canada**                        **2016**
- Epigenetics Conference Travel Award